J. Plasma Physics (1997), *vol.* 58, *part* 3, *pp.* 485–519. Printed in the United Kingdom

Shock waves and rarefaction waves in magnetohydrodynamics. Part 1. A model system

R. S. MYONG† and P. L. ROE

W. M. Keck Foundation Laboratory for Computational Fluid Dynamics, Department of Aerospace Engineering, University of Michigan, Ann Arbor, Michigan 48109, USA

(Received 4 February 1997)

The present study consists of two parts. Here in Part 1, a model set of conservation laws exactly preserving the MHD hyperbolic singularities is investigated to develop the general theory of the nonlinear evolution of MHD shock waves. Great emphasis is placed on shock admissibility conditions. By developing the viscosity admissibility condition, it is shown that the intermediate shocks are necessary to ensure that the planar Riemann problem is well-posed. In contrast, it turns out that the evolutionary condition is inappropriate for determining physically relevant MHD shocks. In the general non-planar case, by studying canonical cases, we show that the solution of the Riemann problem is not necessarily unique – in particular, that it depends not only on reference states but also on the associated internal structure. Finally, the stability of intermediate shocks is discussed, and a theory of their nonlinear evolution is proposed. In Part 2, the theory of nonlinear waves developed for the model is applied to the MHD problem. It is shown that the topology of the MHD Hugoniot and wave curves is identical to that of the model problem.

1. Introduction

Acoustic waves in a magnetized fluid can cause both the magnetic field and the fluid velocity to rotate as they pass. In an inviscid theory, the transverse components of these vectors may change instantaneously across an idealized, infinitesimally thin, discontinuity. They have to satisfy certain conservation principles, but the path taken from one state to the other may be irrelevant. In particular, the path is irrelevant in gasdynamics, since the degree of freedom for an ideal gas is 1 in discontinuities. Out of two possible paths (right-running and left-running), only one path will be physically relevant, and it will not be affected by dissipation irrespective of its magnitude. However, the path taken becomes significant in MHD when dissipation is included, which has raised some doubts about the relevance of ideal MHD to real (i.e. dissipative) MHD. This difference can be attributed to the fact that three degrees of freedom are required for discontinuities in MHD, and thus two equilibrium states can be connected by multiple paths containing other equilibrium states, depending on the associated internal structure. Based on this, in particular, it has been questioned whether numerical methods based on solutions

† Present address: NASA Goddard Space Flight Center, Mail Stop 930, Greenbelt, Maryland 20771, USA.

to the ideal Riemann problem are helpful in obtaining physically correct solutions. This question is connected directly to the stability of intermediate shocks, which has been a lingering source of debate for almost 40 years.

The conventional theory of the stability of intermediate shocks is based on the so-called *evolutionary condition*, also known as the *linearized stability condition*. This theory has been developed largely by Akhiezer *et al.* (1959, 1975), Akhiezer and Polovin (1960), Jeffrey and Taniuti (1964), Kantrowitz and Petschek (1966), Polovin and Demutskii (1990) and Blokhin (1994) since De Hoffman and Teller (1950), Bazer and Ericson (1958) and Ericson and Bazer (1960) derived an explicit form of the MHD Rankine-Hugoniot relations. According to this theory, all intermediate shocks are considered non-physical. Using this theory, Gogosov (1961) developed the theory of resolution of an arbitrary discontinuity in MHD, which corresponds to the exact solution of the MHD Riemann problem. But these works are far from solving the question of which of the multitude of MHD shocks can exist in the real world (Sutton and Sherman 1965, pp. 338–339), since it is known that if only evolutionary shocks are employed, not all Riemann problems have solutions (Jeffrey and Taniuti 1964, pp. 256–259; Polovin and Demutskii 1990, pp. 151–157).

Recently, this theory has been challenged by numerical experiments and theoretical work. From numerical solutions of resistive MHD equations (Wu 1987, 1988*a*,*b*, 1990, 1995; Wu and Kennel 1992, 1993), Wu showed that at least some of the intermediate shocks are admissible and can be formed through nonlinear steepening from continuous waves in the planar problem, contrary to the evolutionary theory. Using a graphical representation of the MHD Rankine–Hugoniot conditions, Kennel *et al.* (1989) elucidated the conditions under which intermediate shocks can be found. But these works are largely based on numerical examples, and therefore are far from giving a general proof of the results on intermediate shocks.

In this paper, we try to clarify the issue by studying a model set of conservation laws exactly preserving the MHD hyperbolic singularities. In this model, only waves propagating to the right with respect to the fluid are represented, which is similar to the piston problem. Nevertheless, both fast, slow and Alfvén waves appear, and there is a singular state, corresponding to magnetosonic conditions, where all three wave speeds are equal, and where the eigenvectors of the fast and slow waves coincide. This creates a degeneracy in the wave structure, topologically identical with that in the full MHD equations. Associated with the non-planar model is a reduced model in which the transverse vector is restricted to remaining on the same plane. In this limit, changing the direction of the transverse vector is done by changing the sign of the transverse vector. We call this the *planar problem*. This problem belongs to the family of 2×2 systems studied by Isaacson *et al.* (1988) and Schaeffer and Shearer (1987*a*), as part of a general programme to classify quadratic degeneracies. For the case of interest here, a complete solution to the Riemann problem is given by Isaacson *et al.* (1988), and we draw heavily on their results. Their solution features a variety of *exotic shocks* or *intermediate shocks* in MHD terms, into which characteristics of more than one family may converge (*overcompressive shocks*), or to which the characteristics of one particular family may run parallel on one side (*compound waves*). Nevertheless, the Riemann problem is uniquely solvable when these waves are included, and it is possible to classify all of the cases that may arise. The essential contribution from this study is that one can determine exactly which types of discontinuity must be admitted to yield a well-posed mathematical problem.

The non-planar model admits as formal solutions all waves found in the planar problem, together with Alfvén waves that rotate the solution vector from one plane to another, resulting in the ill-posedness of the non-planar Riemann problem. In particular, we shall argue that time-independent intermediate shocks can exist in the real world, but are exceptional. They are unstable to any non-coplanar variation on the upstream and downstream states, so that the large-time solution contains only regular shocks. However, these intermediate shocks may persist for long times if they are created from suitable initial conditions and are not strongly perturbed. In addition to these time-independent intermediate shocks, time-dependent intermediate shocks are needed in many cases to explain small-time behaviour.

The methods in this paper are mostly mathematical in nature, causing some difficulties for the reader of this paper with an unfamiliar mathematical language. Part of reason for this difficulty is related to the fact that most previous works are based on physical arguments rather than mathematical analysis. But we find that there is no other way to present our theory without the help of recent mathematical theories on non-strictly hyperbolic conservation laws. To make this paper self-contained, we try to give all elements, but for simplicity leave some details to a reference (Myong 1996).

One of the main reasons for much confusion on the stability of MHD intermediate shocks rests on the misinterpretation of the well-posedness of the mathematical system to the corresponding physical system. The problem is said to be *well-posed* (otherwise, *ill-posed*) if the three criteria (existence, uniqueness and continuous dependence on the data) are satisfied (Stakgold 1979). It has been solid dogma that every mathematical problem approximating a real physical problem should be well-posed. This dogma was successfully applied to various physical systems, for example, gasdynamics. But it is now understood that ill-posed problems occur frequently in practice (three-phase flow in porous media (Holden 1987) and anisotropic plasmas (Kato and Taniuti 1966)) and their physical interpretation and mathematical solutions are somewhat more delicate. *Based on this development, we argue that the ill-posedness of a mathematical problem approximately describing a physical problem does not necessarily violate the well-posedness of the physical problem.* The ill-posedness in this case simply means that there may exist other missing physical effects that have to be included in formulating a mathematical problem. Therefore a fundamental requirement in MHD on physical grounds that solutions must have neighbouring solutions corresponding to a small change of physical properties in the boundary conditions (for example, an arbitrarily small angle of rotation of the plane of the magnetic field (Kantrowitz and Petschek 1966, p. 177)), does not have to be strictly satisfied in the mathematical framework of ideal MHD, since the ideal MHD problem – the Riemann problem or the piston problem in our case – might be ill-posed. Put in another way, other physical effects must be taken into account to satisfy such a requirement. *Thus the logical approach to the MHD problem is to study the well-posedness of various subproblems (hydrodynamic, parallel, planar, coplanar and non-coplanar limits) rather than to try to apply the requirement to the questionable non-planar problem.* Therefore we employ a different fundamental requirement that the solutions of subproblems should match at the boundary. In this approach, no condition is imposed on whether global solutions may depend on internal structure through physical effects.

In Part 2 (Myong and Roe 1997), using this approach, we present MHD Hugoniot and wave curves for planar problems in a phase space essentially comprising the

pressure and the transverse magnetic field. In such a plot, left- or right-moving waves are indistinguishable, so that we essentially study one half of the Riemann problem. The topology of these curves is identical with that of the model. This strongly suggests that MHD shocks should be considered admissible under exactly the same conditions found for the model.

This paper is organized as follows. In Sec. 2, we identify the MHD singularities and study mathematical properties near these points. In Sec. 3, we derive model systems that exactly preserve the MHD singularities. In Sec. 4, by developing shock admissibility conditions, we show the well-posedness of the planar Riemann problem. In order to explain the failure of the evolutionary condition, a limiting case in which the transverse components of the magnetic field vanish on both sides of a shock is considered in detail. In Sec. 5, we identify a fundamental difference between planar problems and non-planar problems and show that the Riemann problem is ill-posed in a non-planar world. Finally, in Sec. 6, we discuss the implication of the new results based on one-dimensional physics.

2. MHD hyperbolic singularities

If there are no external forces, the non-ideal MHD equations take the form, in the one-dimensional problem,

$$\begin{pmatrix} \rho \\ \rho\mathbf{u} \\ \mathbf{B}_\perp \\ E \end{pmatrix}_t + \begin{pmatrix} \rho u \\ \rho\mathbf{u}\mathbf{u} + \mathbf{I}(p + \frac{1}{2}\mathbf{B}_\perp \cdot \mathbf{B}_\perp) - B_x\mathbf{B}_\perp \\ \mathbf{B}_\perp u - B_x\mathbf{v} \\ (E + p + \frac{1}{2}\mathbf{B}_\perp \cdot \mathbf{B}_\perp)u - B_x(\mathbf{B}_\perp \cdot \mathbf{v}) \end{pmatrix}_x = \begin{pmatrix} 0 \\ \mathbf{D}_1\mathbf{u} \\ \mathbf{D}_2\mathbf{B}_\perp \\ \Sigma + \kappa T \end{pmatrix}_{xx}, \quad (2.1)$$

where $\mathbf{B}_\perp$ and $\mathbf{v}$ are the transverse components of the magnetic and velocity fields, and Σ denotes $\frac{1}{2}(\mu u^2 + \nu\mathbf{v} \cdot \mathbf{v} + \eta\mathbf{B}_\perp \cdot \mathbf{B}_\perp)$. $\mathbf{D}_1$ and $\mathbf{D}_2$ are defined as

$$\mathbf{D}_1 = \begin{pmatrix} \mu & 0 & 0 \\ 0 & \nu & 0 \\ 0 & 0 & \nu \end{pmatrix}, \qquad \mathbf{D}_2 = \begin{pmatrix} \eta & -\chi \\ \chi & \eta \end{pmatrix}. \quad (2.2)$$

The longitudinal viscosity μ, the shear viscosity ν, the magnetic resistivity η and the thermal conductivity κ are the main dissipative coefficients, while the Hall coefficient χ is an important dispersive coefficient. By means of the divergence-free condition for the magnetic field, B_x is constant in the one-dimensional problem. The total energy E is defined as $E = \frac{1}{2}\rho\mathbf{u} \cdot \mathbf{u} + p/(\gamma - 1) + \frac{1}{2}\mathbf{B}_\perp \cdot \mathbf{B}_\perp$. By the ideal-gas assumption, $p = \rho RT$. γ is the ratio of specific heats, and is equal to $\frac{5}{3}$ for a monatomic gas.

The MHD equations can be put into Lagrangian form. If we denote the specific volume by τ and define a material coordinate ξ as

$$\xi = \int_{x(t)}^{x} \rho(s,t)\, ds, \quad (2.3)$$

where $x(t)$ is a particle path satisfying $x'(t) = u(x(t), t)$, the MHD equations become

$$\begin{pmatrix} \tau \\ \mathbf{u} \\ \tau\mathbf{B}_\perp \\ e_t \end{pmatrix}_{t'} + \begin{pmatrix} -u \\ \mathbf{I}(p + \frac{1}{2}\mathbf{B}_\perp \cdot \mathbf{B}_\perp) - B_x\mathbf{B}_\perp \\ -B_x\mathbf{v} \\ (p + \frac{1}{2}\mathbf{B}_\perp \cdot \mathbf{B}_\perp)u - B_x(\mathbf{B}_\perp \cdot \mathbf{v}) \end{pmatrix}_\xi = \begin{pmatrix} 0 \\ \mathbf{D}_1\mathbf{u}_x \\ \mathbf{D}_2\mathbf{B}_{\perp x} \\ (\Sigma + \kappa T)_x \end{pmatrix}_\xi, \quad (2.4)$$

where $\tau E = e_t$ and t' indicates a time in the Lagrangian description.

The MHD system yields seven types of wave motion whose speeds relative to the fluid velocity $\lambda_i - u$ are

$$0, \quad \pm c_s, \quad \pm c_a, \quad \pm c_f, \tag{2.5}$$

where $c_a = B_x/\rho^{1/2}$, and $c_{f,s}$ are the fast and slow magnetoacoustic wave speeds, given by

$$2c_{f,s}^2 = a^2 + \frac{\mathbf{B}\cdot\mathbf{B}}{\rho} \pm \left\{ \left(a^2 + \frac{\mathbf{B}\cdot\mathbf{B}}{\rho} \right)^2 - 4a^2 c_a^2 \right\}^{1/2}. \tag{2.6}$$

Here the acoustic wave speed a is given by $a^2 = \gamma p/\rho$ for an ideal gas.

The first wave, which moves with the fluid velocity, is the entropy wave. It is well known that entropy and Alfvén waves are associated with linearly degenerate characteristic fields ($\nabla\lambda_i \cdot \mathbf{r}_i = 0$ for all phase space, where λ_i and $\mathbf{r}_i$ represent the eigenvalues and the right eigenvectors associated with i-waves), while slow and fast magnetoacoustic waves are associated with nonlinear characteristic field ($\nabla\lambda_i \cdot \mathbf{r}_i$ not generally zero). However, $\nabla\lambda_i \cdot \mathbf{r}_i$ may change sign, and is zero for certain critical states. This implies that the associated characteristic speeds for the magnetoacoustic waves are not convex.

In addition to the *non-convexity*, there are chances that these wave speeds are not distinct. When $\mathbf{B}_\perp \cdot \mathbf{B}_\perp = 0$,

$$c_s^2 = c_a^2, \quad c_f^2 = a^2 \quad \text{for } a^2 > c_a^2, \tag{2.7}$$

$$c_f^2 = c_a^2, \quad c_s^2 = a^2 \quad \text{for } a^2 < c_a^2. \tag{2.8}$$

In this case, the Alfvén wave interacts or resonates with one of the magnetoacoustic waves. In particular, when $\mathbf{B}_\perp \cdot \mathbf{B}_\perp = 0$ and $c_a^2 = a^2$,

$$c_s^2 = c_a^2 = c_f^2 = a^2. \tag{2.9}$$

This point is called the *triple umbilic point*. This represents the interaction of an Alfvén wave and slow, fast magnetoacoustic waves. Note that this triple umbilic point becomes a *double umbilic point* in the planar problem with variables (ρ, u, v, B_y, p), and such a point represents the interaction of slow, fast magnetoacoustic waves at $c_a^2 = a^2$.

The MHD singularity looks like a straight string corresponding to the $a^2 - c_a^2$ axis in a space $(a^2 - c_a^2, B_y, B_z)$. The resonances have a profound effect on the construction of weak solutions to the hyperbolic conservation laws. Hyperbolic conservation laws with wave resonances are called *non-strictly hyperbolic*, and were studied extensively in the 1980s by Keyfitz and Kranzer (1980), Schaeffer and Shearer (1987*a*,*b*), Shearer *et al.* (1987) and Isaacson and Temple (1988*a*,*b*), as mathematical models describing elasticity and oil recovery.

3. Derivation of model systems

Model systems that preserve the MHD singularity and are easier to deal with can be derived from the full MHD equations. Brio and Rosenau (1994) developed a 3×3 model system in order to investigate MHD shocks, using the perturbation method. But we can also obtain the same system by physical reasoning alone. A close look of MHD waves suggests that the MHD wave structure near the triple umbilic point can be revealed in a three-dimensional phase space consisting of p, B_y and B_z. In other words, the nonlinear interactions can be explained by one-directional waves

(either purely left-running waves or purely right-running waves), because six waves are symmetric about the entropy wave moving with the fluid particle. To this end, the MHD system is *symmetrically non-strictly hyperbolic*. Therefore a 3×3 model system preserving the singularity can be derived by considering only the momentum equation of u and the conservation laws of the magnetic fields. The mass conservation law and energy equation are largely associated with the entropy wave, and momentum equations of v and w are related by the conservation laws of B_y and B_z. The resulting equations are, starting from the Lagrangian form,

$$\begin{pmatrix} u \\ \tau B_y \\ \tau B_z \end{pmatrix}_{t'} + \begin{pmatrix} p + \frac{1}{2}(B_y^2 + B_z^2) \\ -B_x v \\ -B_x w \end{pmatrix}_{\xi} = \begin{pmatrix} \mu u_x \\ \eta B_{y_x} - \chi B_{z x} \\ \chi B_{y_x} + \eta B_{z x} \end{pmatrix}_{\xi}, \tag{3.1}$$

with $\tau_{t'} = u_\xi$. Let us assume

$$B_x = 1, \quad \tau \approx 1, \quad v \approx B_y, \quad w \approx B_z. \tag{3.2}$$

Noting that u has the same order of magnitude as a and thus $p \approx u^2$, the system of three equations reduces to the 3×3 model system developed by Brio and Rosenau (1994):

$$\mathbf{u}_t + \mathbf{f}_x = \mathbf{D}\mathbf{u}_{xx}, \tag{3.3}$$

where

$$\mathbf{u} = \begin{pmatrix} u \\ B_y \\ B_z \end{pmatrix}, \ \mathbf{f} = \begin{pmatrix} \frac{1}{2}(cu^2 + {B_y}^2 + {B_z}^2) \\ (u-1)B_y \\ (u-1)B_z \end{pmatrix}, \ \mathbf{D} = \begin{pmatrix} \mu & 0 & 0 \\ 0 & \eta & -\chi \\ 0 & \chi & \eta \end{pmatrix}. \tag{3.4}$$

Here u represents a thermodynamic property. The parameter c controls the behavior of the whole system, and Brio and Rosenau set its value equal to $\gamma + 1$, although they omitted the proof (Web *et al.* 1995).

In order to transform the system into a mathematically more manageable form, we need the key step to relate the study of the MHD singularity with the recent mathematical works on 2×2 quadratic hyperbolic conservation laws. Let us consider the Taylor series of $f(\mathbf{u})$ about a triple umbilic point $\mathbf{u}^* = (1/(1-c), 0, 0)$ (Schaeffer and Shearer 1987*a*):

$$f(\mathbf{u}) = f(\mathbf{u}^*) + df(\mathbf{u}^*)(\mathbf{u} - \mathbf{u}^*) + q(\mathbf{u} - \mathbf{u}^*) + \text{h.o.t.}, \tag{3.5}$$

where q: $\mathbf{R}^3 \to \mathbf{R}^3$ is a homogeneous quadratic mapping and h.o.t. represents the remainder. The truncated series $f_T(\mathbf{u})$ is

$$f(\mathbf{u}^*) + df(\mathbf{u}^*)(\mathbf{u} - \mathbf{u}^*) + q(\mathbf{u} - \mathbf{u}^*). \tag{3.6}$$

In this case the following two relations are satisfied:

$df(\mathbf{u}^*)$ is diagonalizable;

$df_T(\mathbf{u})$ has distinct eigenvalues for all $\mathbf{u} \in \mathbf{R}^3 - \mathbf{u}^*$.

Then the system can be simplified by the following steps. First, the system (3.3) is unchanged on replacing $f(\mathbf{u}) - f(\mathbf{u}^*)$ by $f(\mathbf{u})$. Next, using the first relation we have $df(\mathbf{u}^*) = \lambda \mathbf{I}$ for $\lambda = c/(1-c)$. Therefore the linear terms in (3.6) can be eliminated by the change of variable $x' = x - \lambda t$. Finally, it does not matter if we replace $\mathbf{u} - \mathbf{u}^*$ by $\mathbf{u}$ and apply a transformation $\mathbf{u} = 2\mathbf{u}'$. Therefore, if v and w are used to represent B_y and B_z, the nonlinear features in the system (3.3) can be represented

by purely quadratic equations:

$$\begin{pmatrix} u \\ v \\ w \end{pmatrix}_t + \begin{pmatrix} cu^2 + v^2 + w^2 \\ 2uv \\ 2uw \end{pmatrix}_x = \begin{pmatrix} \mu & 0 & 0 \\ 0 & \eta & -\chi \\ 0 & \chi & \eta \end{pmatrix} \begin{pmatrix} u \\ v \\ w \end{pmatrix}_{xx}. \tag{3.7}$$

Surprisingly, the planar restriction of this *non-planar model system* is nothing but the 2×2 quadratic system of non-strictly hyperbolic conservation laws developed by Isaacson *et al.* (1988) and Schaeffer and Shearer (1987*a*):

$$\begin{pmatrix} u \\ v \end{pmatrix}_t + \begin{pmatrix} cu^2 + v^2 \\ 2uv \end{pmatrix}_x = \begin{pmatrix} \mu & 0 \\ 0 & \eta \end{pmatrix} \begin{pmatrix} u \\ v \end{pmatrix}_{xx}. \tag{3.8}$$

We call this system the *planar* 2×2 *model*. It will be used to study the planar MHD problem. Schaeffer and Shearer showed that the wave structure of the system (3.8) is distinguished by four different cases (I: $c < 0$; II: $0 < c < 1$; III: $1 < c < 2$; IV: $2 < c$). By comparing the planar model with the 5×5 MHD system, we can prove that

$$c = \gamma + 1, \quad u = \left(\frac{a}{c_a}\right)^2 - 1, \quad v = \frac{B_y}{B_x}, \quad w = \frac{B_z}{B_x}. \tag{3.9}$$

The details of this proof are given in Part 2 (Myong and Roe 1997). The first condition implies that the topology of the MHD wave structure is identical with that of wave structure of case IV in the quadratic system.

We can derive another model system by considering the second and third equations of the system (3.7). Let us assume that u is balanced by the transverse fields through

$$u = \tfrac{1}{2}(v^2 + w^2). \tag{3.10}$$

Note, however, that under this assumption u always has a positive value, which restricts its application to MHD since u can have any sign in the 3×3 model. Then, the system reduces to

$$\begin{pmatrix} v \\ w \end{pmatrix}_t + \begin{pmatrix} (v^2 + w^2)v \\ (v^2 + w^2)w \end{pmatrix}_x = \begin{pmatrix} \eta & -\chi \\ \chi & \eta \end{pmatrix} \begin{pmatrix} v \\ w \end{pmatrix}_{xx}. \tag{3.11}$$

We call this system the *rotational* 2×2 *model*. This is a rotationally degenerate system of conservation laws with the cubic flux function and is similar to the CKB (Cohen–Kulsrud–Burgers) system (Kennel *et al.* 1990), which describes the interaction of an Alfvén wave and a magnetoacoustic wave. It is known as the derivative nonlinear Schrödinger equation (DNLS) when $\eta = 0$. It also belongs to the Keyfitz–Kranzer model, which has been studied as a model of an elastic string (Keyfitz and Kranzer 1980) and for multi-phase flow (Isaacson *et al.* 1990).

4. Planar model system

The planar 2×2 model system may be written as

$$\mathbf{u}_t + \mathbf{f}_x = \mu \mathbf{u}_{xx}, \tag{4.1}$$

where

$$\mathbf{u} = \begin{pmatrix} u \\ v \end{pmatrix}, \ \mathbf{f} = \begin{pmatrix} cu^2 + v^2 \\ 2uv \end{pmatrix}, \tag{4.2}$$

and $2 < c$, if it is assumed that $\mu = \eta$. The waves will be described as slow and fast; their speeds are given by

$$\lambda_{f,s} = (c+1)u \pm \{(c-1)^2u^2 + 4v^2\}^{1/2}, \tag{4.3}$$

always satisfying $\lambda_s \leqslant \lambda_f$, and the right eigenvectors are

$$\mathbf{r}_{f,s} = \begin{pmatrix} \lambda_{f,s} - u \\ v \end{pmatrix}. \tag{4.4}$$

When $u = v = 0$, all wave speeds vanish simultaneously, and the eigenvectors are indeterminate even when normalized. Also, the construction of the rarefaction wave breaks down if the wave speeds λ_i have extreme values on integral curves of $\mathbf{r}$. This condition can be expressed in mathematical terms as $\boldsymbol{\nabla}\lambda \cdot \mathbf{r} = 0$. In the planar 2×2 model, it is satisfied on the $v = 0$ axis.

4.1. Rankine–Hugoniot relations

Travelling shock-wave solutions

$$\mathbf{u}(x,t) = \begin{cases} \mathbf{u}_L & \text{if } x < st, \\ \mathbf{u}_R & \text{if } x > st \end{cases}$$

are characterized by the Hugoniot waves $[\mathbf{f}] = s[\mathbf{u}]$. For the planar model system, they are

$$s\,[u] = 2c\bar{u}\,[u] + 2\bar{v}\,[v], \tag{4.5}$$

$$s\,[v] = 2\bar{v}\,[u] + 2\bar{u}\,[v], \tag{4.6}$$

where the overbars indicate arithmetic averages taken across the discontinuity and $[Q]$ denotes the jump in a quantity Q, that is, $Q_R - Q_L$. The Rankine–Hugoniot relation is obtained by eliminating s; it is

$$\bar{v}\,[u]^2 + (1-c)\bar{u}\,[u][v] - \bar{v}\,[v]^2 = 0. \tag{4.7}$$

If the state on one side, say the left, is taken as given then this equation is cubic in v_R and quadratic in u_R. Because the equation is homogeneous, the shape of the curve depends only the ratio v_L/u_L. There is a horizontal asymptote at the value $v_{\max}/v_L = c/(c-2)$, and a loop that passes around the origin. The highest and lowest points on the Hugoniot are given by

$$v = \frac{v_L}{c-2} \pm \frac{c-1}{c-2}\{v_L^2 + (c-2)\,u_L^2\}^{1/2}. \tag{4.8}$$

Figure 1 displays the Hugoniot curves for five cases. In all our illustrations we have taken $c = \frac{8}{3}$, corresponding to $\gamma = \frac{5}{3}$. These cases are chosen because there is an aspect of the curves that depends on where the state $\mathbf{u}_L$ lies with respect to the critical lines $v^2/u^2 = c$ on which one of the wave speeds vanishes. This aspect is the way that the Hugoniot curve divides into sections corresponding to different types of discontinuity.

4.2. Shock waves

In addition to the Rankine–Hugoniot jump conditions, supplementary conditions are needed to determine which jumps are physically admissible. Before considering such conditions, it is very useful to classify the discontinuities by how many characteristics enter them from each side. For a travelling shock, the signs of the

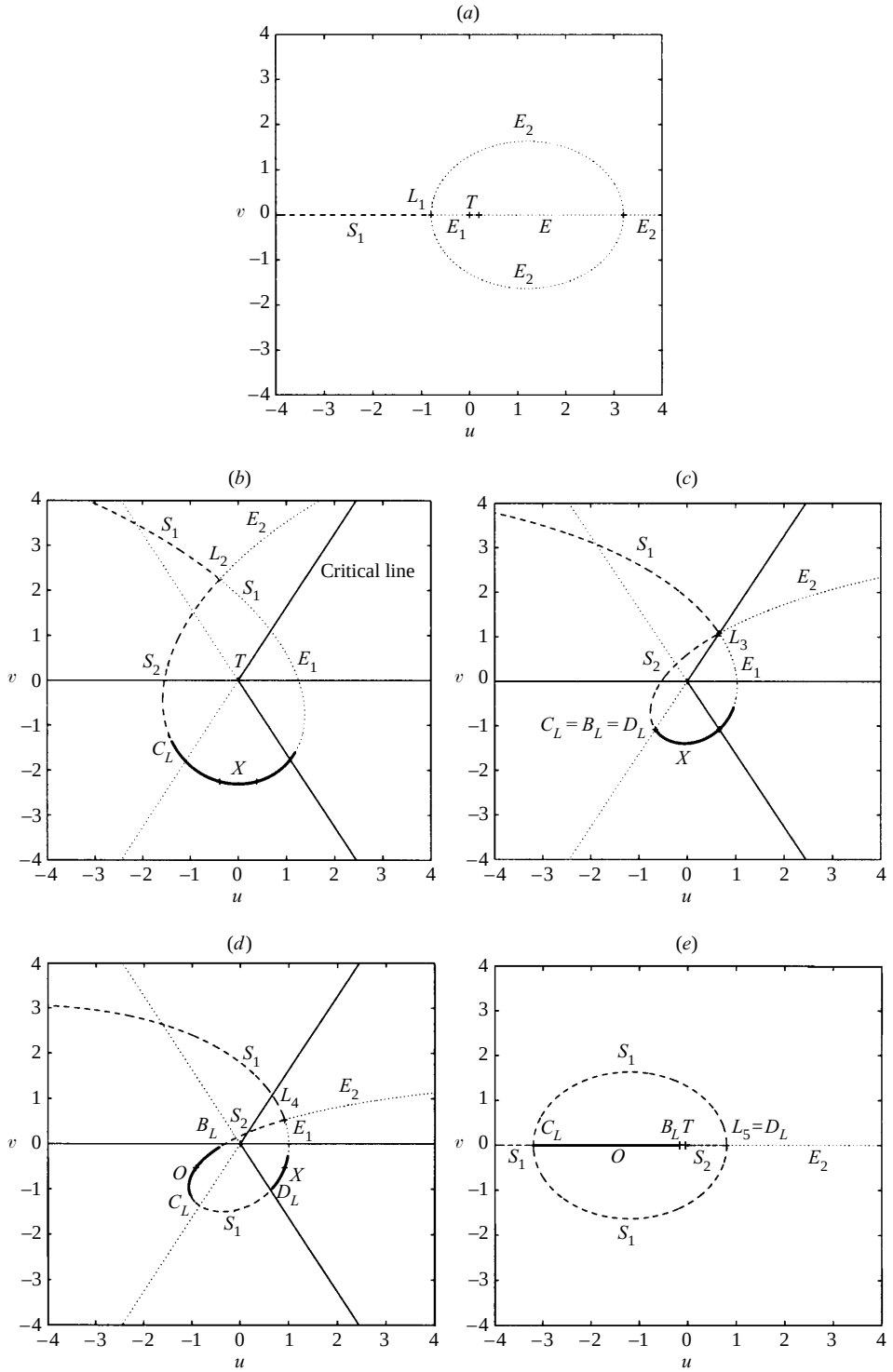

Figure 1. Hugoniot loci and shock type: S_1, S_2 slow, fast; E_1, E_2, slow, fast expansive; E, expansive; O, overcompressive; X, undercompressive shocks. C_L, B_L and D_L are critical points, which will be explained in Sec. 4.6. T represents the umbilic point.

Table 1. Types of shocks according to the sign of four parameters: S_1, S_2, slow, fast; E_1, E_2, slow, fast expansive; O, X, overcompressive, undercompressive; E, expansive; R_t, L_t, right, left transport shocks.

Parameter/shock	S_1	E_1	S_2	E_2	O	E	X	R_t	L_t
P_1	+	+	−	+	−	+	+	+	−
P_2	+	−	+	+	+	−	+	−	+
P_3	+	+	+	−	+	−	+	+	−
P_4	−	+	+	+	−	+	+	−	+

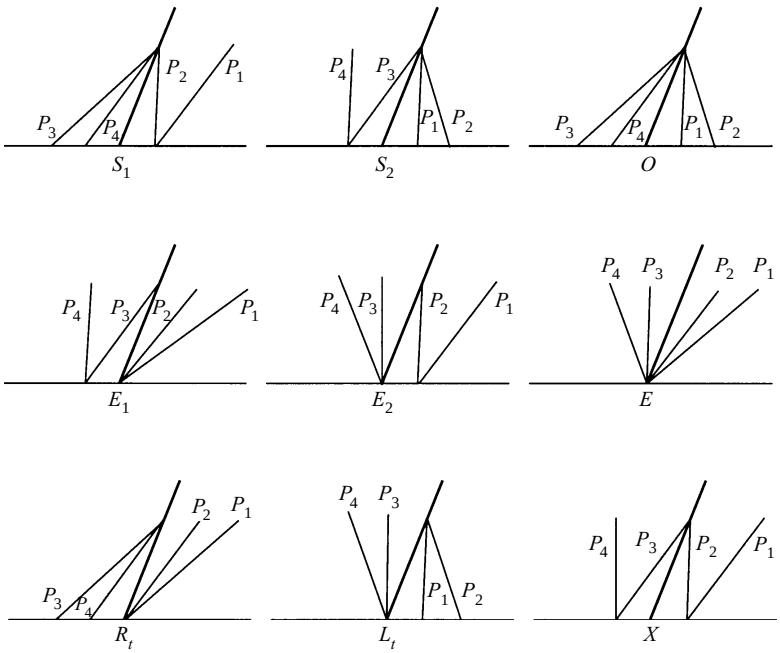

Figure 2. Shock classification according to the sign of four parameters in (x, t) space: S_1, S_2, slow, fast; E_1, E_2, slow, fast expansive; O, X, overcompressive, undercompressive; E, expansive; R_t, L_t, right, left transport shocks. The thick line represents a travelling shock, and the thin lines represent characteristics.

following four parameters determine which of the slow, fast characteristics run into the shock:

$$P_1 = \lambda_f - s, \quad P_2 = s - \lambda_s, \quad P_3 = \lambda_{fL} - s, \quad P_4 = s - \lambda_{sL}. \tag{4.9}$$

There are 16 possible sign distributions of discontinuities of these four parameters, but only 9 can actually arise because the following relations must be satisfied:

$$c_s \leqslant c_f, \quad c_{sL} \leqslant c_{fL}. \tag{4.10}$$

In Table 1 we classify nine types of shocks according to the signs of these parameters. Subscripts 1 and 2 indicate slow and fast waves respectively. The relationship between the speed of a shock and characteristics in nine types of shocks is summarized in Fig. 2. The different types of shocks occurring in the planar 2×2 model system are illustrated in Fig. 1.

4.2.1. Slow, fast shocks.. For just one of the families f, s it is true that the Lax condition

$$\lambda_R < s < \lambda_L \tag{4.11}$$

holds, so that the shock arises from coalescing waves of that family. Shock jumps corresponding to slow waves are labelled S_1 in the diagrams, and jumps corresponding to fast waves are labelled S_2. S_1 and S_2 in the upper half-plane of Fig. 1 correspond to III→IV and I→II shocks for the non-planar MHD problem, while those in the lower half-plane correspond to II→IV and I→III intermediate shocks (see Sec. 5.2).

4.2.2. Expansion shocks.. These occur when the above inequality holds with signs reversed. These branches are labelled E, E_1 and E_2.

4.2.3. Overcompressive shocks.. The above inequality is true for both families. They are I→IV intermediate shocks in MHD. They can be regarded as belonging to either family. It can be shown that the Hugoniot contains overcompressive shocks (labelled O) only if the left state lies in the region $|v_L/u_L| < c^{1/2}$. Then a particular example (with $s = 0$) of an overcompressive shock is found by taking $u = -u_L$ and $v = -v_L$.

4.2.4. Undercompressive shocks.. For these (labelled X), we have

$$\lambda_{s,L} < s < \lambda_{f,L}, \tag{4.12}$$

$$\lambda_{s,R} < s < \lambda_{f,R}. \tag{4.13}$$

MHD II→III intermediate shocks are of this type. They are also called *crossing shocks*, since the fast and slow characteristics cross each other at the shock.

4.3. Rarefaction waves

From the right eigenvectors, the integral curves are defined by

$$\left.\frac{dv}{du}\right|_{f,s} = \frac{v}{\frac{1}{2}\lambda_{f,s} - u}, \tag{4.14}$$

which are the paths taken in phase space, as the solution traverses a simple wave, and have the general appearance shown in Fig. 3. Invariants for integral curves can be calculated by introducing

$$u = r\cos\theta = \frac{2}{c-1}\, r'\cos\theta', \quad v = r\sin\theta = r'\sin\theta'. \tag{4.15}$$

Then we have

$$\frac{r'^2(\cos\theta' \pm 1)^{(c-1)/(c-2)}}{\{(3-c)\cos\theta' \pm (c-1)\}^{(3-c)/(c-2)}} = \text{const}, \tag{4.16}$$

with

$$\tan\theta = \frac{c-1}{2}\tan\theta', \quad \frac{r^2}{r'^2} = \frac{4}{(c-1)^2}\cos^2\theta' + \sin^2\theta'. \tag{4.17}$$

Here + and − indicate slow and fast waves respectively. When $c > 2$, these integral curves are similar to the parabola. If the curves are followed from left to right in physical space in the direction of increasing u, the characteristics form diverging fans, and represent rarefaction waves.

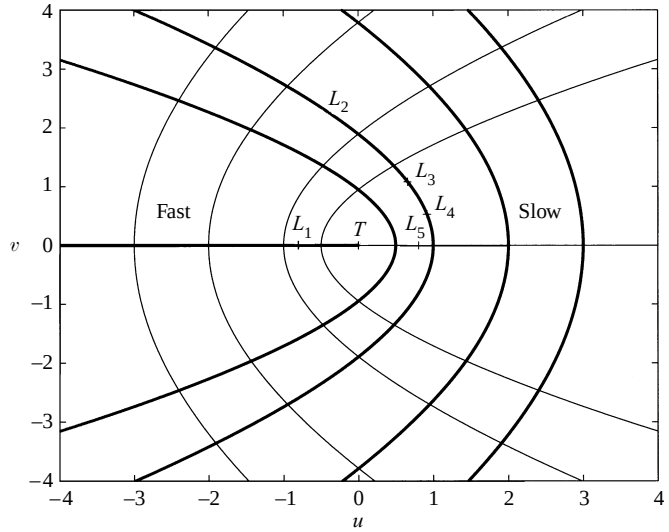

Figure 3. Integral curves. The thick lines indicate slow rarefaction waves, and the thin lines indicate fast rarefaction waves. T denotes the umbilic point and $L_{1,2,3,4,5}$ represent the five left states in the Hugoniot curves.

4.4. Shock admissibility conditions

In order to select physically admissible shocks, supplementary conditions are imposed on jumps. In gasdynamics, various conditions, for example the Lax condition and the entropy-flux condition, work well and they all turn out to be equivalent. However, a simple extension of such conditions to jumps that are not always associated with a particular characteristic family is not straightforward. They may become different, and some can be inappropriate or over-restrictive. Up to now, several shock admissibility conditions have been proposed (Freistühler 1992; Keyfitz 1995). In this section such conditions will be applied to the model system in which genuine nonlinearity fails and eigenvalues are not distinct everywhere: the geometric entropy condition (or Lax condition), the entropy-flux criterion, the viscosity admissibility criterion (Gomes 1989), linearized stability condition (Akhiezer *et al.* 1959; Blokhin 1994), and nonlinear stability and asymptotic stability conditions (Liu 1992). The first condition is based solely on the simple geometric interpretation, while the next two and three conditions are formulated as physical principles and self-contained analysis. Emphasis will be place on which conditions are suitable for obtaining the well-posedness.

4.4.1. Geometric condition.. For an $n \times n$ system, the Lax condition (Lax 1957) is

$$\lambda_i(\mathbf{u}_R) < s < \lambda_i(\mathbf{u}_L) \tag{4.18}$$

for a shock of the i-family. For the 2×2 system, physically relevant shocks satisfy

$$\lambda_s(\mathbf{u}_R) < s < \lambda_s(\mathbf{u}_L), \quad s < \lambda_f(\mathbf{u}_R), \tag{4.19}$$

$$\lambda_f(\mathbf{u}_R) < s < \lambda_f(\mathbf{u}_L), \quad s > \lambda_s(\mathbf{u}_L). \tag{4.20}$$

It should be mentioned that this theory was developed for a system with real and distinct eigenvalues. For a scalar conservation law with convex flux function, it

reduces to

$$\lambda(u_R) < s < \lambda(u_L). \tag{4.21}$$

4.4.2. Physical conditions.. The entropy-flux condition can be formulated as

$$\iint (e_t + h_x)\, dx\, dt \leqslant 0, \tag{4.22}$$

where e is a convex entropy function and h is the entropy flux. For the 2×2 system, e and h can be defined as $\frac{1}{2}(u^2 + v^2)$ and $2u(\frac{1}{3}cu^2 + v^2)$, respectively. For all compressive waves, $u_L > u_R$, meaning that the entropy always increases through physical shock waves (see Sec. 5.3.2).

The viscosity admissibility condition requires that physically admissible shocks satisfying the Rankine–Hugoniot conditions be those that can be approximated by the travelling-wave solutions to the associated parabolic system. That is, a shock wave $x = st$ joining states $\mathbf{u}_L$ and $\mathbf{u}_R$ has a viscous profile if the system has a solution of the form

$$\mathbf{u} = \mathbf{u}(\xi \equiv (x - st)/\mu) \quad \text{satisfying} \quad \mathbf{u}(\xi = -\infty) = \mathbf{u}_L \quad \text{and} \quad \mathbf{u}(\xi = \infty) = \mathbf{u}_R. \tag{4.23}$$

Then we have a dynamical system that could be used to establish the existence of heteroclinic orbits. The procedure of developing the viscosity admissibility condition will be explained in detail later.

4.4.3. Self-contained conditions.. The linearized stability condition on a uniform shock is formulated as follows (Jeffrey and Taniuti 1964). Let us consider inviscid perturbation of a uniform shock

$$\mathbf{u}^o(x,t) = \begin{cases} \mathbf{u}^o_- & \text{if } x < s_o t, \\ \mathbf{u}^o_+ & \text{if } x > s_o t. \end{cases}$$

Across the shock, the following jump relations must be satisfied:

$$\mathbf{f}(\mathbf{u}^o_+) - \mathbf{f}(\mathbf{u}^o_-) = s_o(\mathbf{u}^o_+ - \mathbf{u}^o_-). \tag{4.24}$$

Assuming that the shock is perturbed by small-amplitude waves impinging from both sides, we have the following perturbation data:

$$\mathbf{u}_\pm(x,0) = \mathbf{u}^o_\pm(x) + \varepsilon \sum_{p=1}^{p_{\text{in}}} \mathbf{v}^p_\pm(x)\mathbf{r}^p_\pm, \quad \varepsilon \ll 1, \tag{4.25}$$

if we decompose the perturbed components in an eigenvector expansion. $\mathbf{r}^p_\pm$ denotes the right eigenvectors of $\mathbf{A}_\pm = \partial\mathbf{f}/\partial\mathbf{u}(\mathbf{u}^o_\pm)$, and $\mathbf{v}^p_\pm$ is the coefficient of $\mathbf{r}^p$ in an eigenvector expansion of the vector $\mathbf{u}(x,t)$. The initial perturbation leads to perturbation of the shock speed and the generation of outgoing waves from the shock.

Next, let us consider the linearized $n \times n$ system on each side of the shock,

$$\mathbf{u}_t + \mathbf{A}(\mathbf{u}_\pm)\mathbf{u}_x = 0. \tag{4.26}$$

The solution can be written as

$$\mathbf{u}_\pm(x,t) = \mathbf{u}^o_\pm + \varepsilon \sum_{p=1}^{n} \mathbf{v}^p_\pm(x - \lambda^p_\pm t, 0)\, \mathbf{r}^p_\pm, \tag{4.27}$$

where $\lambda^p_\pm$ are the characteristic speeds of the linear system in the frame of reference

moving with the shock speed s_o. If we assume the shock to be weak, the perturbation jump relations

$$\mathbf{f}(\mathbf{u}_+) - \mathbf{f}(\mathbf{u}_-) = (s_o + \varepsilon\tilde{s})(\mathbf{u}_+ - \mathbf{u}_-) \tag{4.28}$$

yield a linear system

$$\tilde{s}[\mathbf{u}^o] + \sum_{p=1}^{p_{\text{out}}} \lambda_\pm^p \mathbf{v}_\pm^p (x - \lambda_\pm^p t, 0)\, \mathbf{r}_\pm^p = \sum_{p=1}^{p_{\text{in}}} \lambda_\pm^p \mathbf{v}_\pm^p (x - \lambda_\pm^p t, 0)\, \mathbf{r}_\pm^p \tag{4.29}$$

for the unknowns $p_{\text{out}} + 1$ when incoming distributions are given. *Hence the system has a non-trivial solution only if (1)* $p_{\text{out}} = n - 1$ *and (2) the vectors* $\mathbf{r}_{\text{out}}^p$ *and* $[\mathbf{u}^o]$ *are linearly independent*. Since there are $2n$ waves present, $p_{\text{in}} = n - 1$ and two waves get *lost* in the shock. If these are waves of the same family then this is the Lax condition.

Also, the nonlinear stability condition can be formulated from the linearized stability condition by relaxing the weakness of perturbation on shocks, becoming a nonlinear existence problem that the perturbed data lead to a unique classical solution to the quasilinear problem on each side of the shock.

Finally, the asymptotic stability condition is related to the question of whether the discontinuity evolves from smooth data approximating a uniform shock.

4.4.4. Failure of the linear stability condition.. If eigenvalue is a real, simple, genuinely nonlinear characteristic value at $\mathbf{u}_L$, all these conditions are known to be equivalent to the Lax condition for sufficiently small-amplitude shocks. In particular for a system whose characteristic speeds are all real and distinct, and depend monotonically on the corresponding characteristic variables, the geometric condition and the linear stability condition work well. However, for the 2×2 model system where these non-degeneracy conditions fail, such simple conditions turn out to be inappropriate.

For some non-classical shock types, the system (4.29) becomes insolvable (Brio & Rosenau 1994).

(i) The system has more unknowns than given equations, and thus there are infinitely many possible solutions. For the general quadratic 2×2 system, X, R_t, and L_t are such shocks. (Expansive shocks are also such shocks, but they are obviously inadmissible.) For the 2×2 model system, such insolvability is found only in undercompressive shocks.

(ii) The system is overdetermined and thus it does not have a solution. Overcompressive shocks are such shocks. All characteristics run into the shock.

(iii) The system is invalid when waves move with the shock speed, and thus it cannot be characterized as incoming or outgoing. Such cases can be found in compound waves, which will be explained later.

In conclusion, the linearized stability condition and the geometric condition fail for a scalar equation with non-convex flux function and for a system in which the associated waves are not convex. It is expected that the nonlinear stability condition will give the correct result only if the perturbations are large enough.

4.5. Viscosity admissibility condition

The failure of admissibility criteria based on linear stability theory for non-strictly hyperbolic systems implies that there exist some missing physical effects that have to be taken into account. The most obvious one is dissipation by viscosity or resistivity, so that the viscosity admissibility condition is considered to overcome the limitation of geometric approaches. It is based on the analysis of a dynamical system, which is the essential tool for selecting shocks that admit a viscous profile. The dynamical system is determined by travelling-wave solutions of the associated viscosity equation. Some important theorems of the dynamical system are summarized in the appendix. The dynamical system of the planar problem (4.1) can be written as

$$u_\xi = f(\mathbf{u}) - f(\mathbf{u}_L) - s(u - u_L) \equiv \Theta(\mathbf{u}), \tag{4.30}$$

$$v_\xi = g(\mathbf{u}) - g(\mathbf{u}_L) - s(v - v_L) \equiv \Phi(\mathbf{u}), \tag{4.31}$$

where

$$\mathbf{f} = (f, g) = (cu^2 + v^2, 2uv), \tag{4.32}$$

and $2 < c$. In order to analyse this dynamical system, let us examine first singularities, which will be determined by solving $\Theta = 0$ and $\Phi = 0$ for given s and $\mathbf{u}_L$. The reason for this is that we are interested only in profiles connecting singularities.

In general, singularities on the finite domain are the intersections of two curves (ellipse and hyperbola) defined by $\Theta = \Phi = 0$. In our case we can observe two, three and four singularities. Three singularities occur in a degenerate case. However, there is a special case in which $\mathbf{u}_L$ is the umbilic point, so that eigenvalues become equal. In this case, singularities can be attained by considering the Hugoniot locus (4.7) at the umbilic point ($u_L = v_L = 0$), which is

$$v = 0. \tag{4.33}$$

Hence there are two singularities at infinity independent of s. These singularities can be revealed by the Poincaré transform.

Following the method summarized in the appendix, the Jacobian matrix of the vector field (Θ, Φ) evaluated at the singularities, which can be obtained by applying the Poincaré transformation $u = 1/z$ and $v = y/z$ to the vector field, is

$$\begin{pmatrix} \Gamma'(\alpha) & 0 \\ 0 & \Gamma(\alpha) \end{pmatrix}, \tag{4.34}$$

where

$$\Gamma'(y) = -f(1, y) - yf'(1, y) + g'(1, y), \tag{4.35}$$

$$\Gamma(y) = -f(1, y), \tag{4.36}$$

and $\alpha = 0$ for $2 < c$ (for details see Gomes (1989)). Here $\alpha = 0$ corresponds to the $v = 0$ condition. For $c < 2$, α has three values $\alpha = \pm(2 - c)^{1/2}, 0$, which can be calculated from

$$\alpha f(1, \alpha) - g(1, \alpha) = 0. \tag{4.37}$$

Note that α is the slope of the Hugoniot through the umbilic point, and is equal to y since singularities at infinity ($y, z = 0$), if they exist, satisfy (4.37). To determine the type of singularities at infinity, we consider the sign of $\Gamma(\alpha)\Gamma'(\alpha)$. At $y = 0$, we

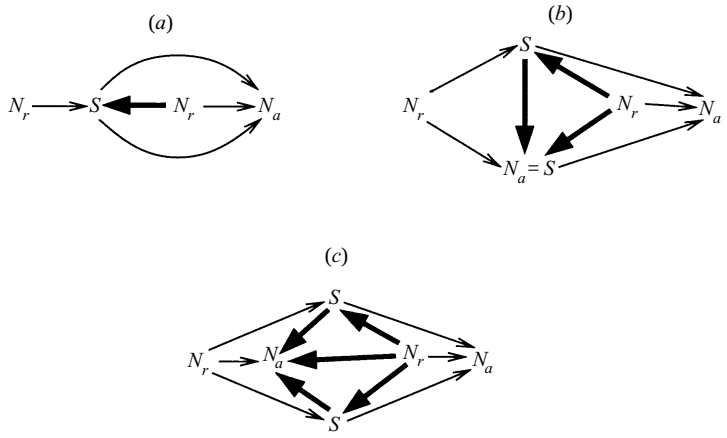

Figure 4. Examples of the global phase portrait of the planar model problem. N_r, N_a and S denote repelling node, attracting node and saddle respectively. The connections from singularities at infinity are shown by thin lines.

have

$$\Gamma'(y)(= 2 - c - 3y^2) = 2 - c, \tag{4.38}$$

$$\Gamma(y)(= -y^2 - c) = -c. \tag{4.39}$$

This indicates that singularities at infinity are two nodes for $2 < c$ (including an antipodal point of the Poincaré sphere).

Once we find singularities, we can determine their type using index theory, without resolving orbits in detail. An important result of index theory is the *Poincaré index theorem*, which shows that the sum of the indices of singularities on a two-dimensional surface is 2 (see the appendix). For four singularities in the finite domain, the index theorem yields $2N - 2S + 2 = 2$ and $N + S = 4$. Then, we obtain two nodes and two saddles as singularities in the finite domain. Similarly, we can find a node and a saddle for two singularities. In the case of three singularities, we have one saddle, one node and a non-hyperbolic saddle–node in which the index is zero. The global phase portraits are given in Fig. 4. It can easily be found that all regular shocks and overcompressive shocks have viscous profiles, since there are saddle–node and node–node connections, but undercompressive shocks do not have viscous profiles, since there is no saddle–saddle connection.

The non-existence of trajectories connecting saddle points has a deep meaning since it assures the structural stability of the planar vector field by Peixoto's theorem (Perko 1993, pp. 292–301). By structural stability, it is meant that the vector field retains its topology under the disturbance. Therefore we can select physically relevant shocks for which the corresponding physical system is structurally stable.

4.6. Compound waves

In Sec. 4.4.4 it was noted that rarefaction waves can move with the shock and in that case the linearized stability theory fails. Here, we introduce *compound waves*, also known as *composite waves*, as substitutes for undercompressive shocks which are inadmissible by the viscous admissibility condition. Historically, these waves are identified in a model for multiphase flow in a porous medium (Bell *et al.* 1986).

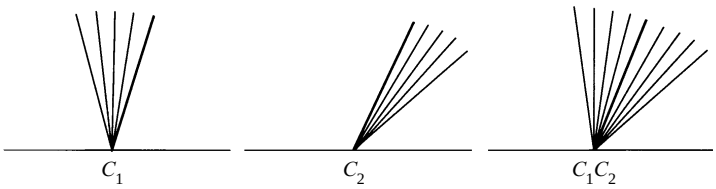

Figure 5. Compound waves in (x,t) space: C_1, C_2, slow, fast compound; C_1C_2, transitional waves. The shock is shown by the thick line, while characteristics are shown by the thin lines.

In MHD, they were first identified by Wu (1987) from the numerical solutions to full MHD.

Here the simplest of this kind of models will be considered in order to show how compound waves are constructed:

$$u_t + (u^3)_x = 0. \tag{4.40}$$

Notice that it corresponds to the equation governing the magnitude of the transverse magnetic field in the rotational 2×2 model. The characteristic speed for this model $\lambda = 3u^2$ which is parabola-like about $u = 0$. For the Riemann problem with the initial data $u_R = -u_L$, $0 < u_L$, the solution can be obtained by constructing the convex hull (LeVeque 1990), that is, the smallest convex set. At u^*, $s^* = \{f(u^*) - f(u_L)\}/(u^* - u_L)$ is identical with $f'(u^*)$, which means that the shock moves as the same speed as the adjacent characteristics. For the planar model, they consist of waves of one family (slow and fast) and are of three types, shown in Fig. 5. There exist critical points in the Hugoniot curves that are very helpful for identifying compound waves. The critical point C_L is defined as the point where the Hugoniot locus is tangent to a fast integral curve, which satisfies

$$\lambda_f(\mathbf{u}) - s(\mathbf{u}_L, \mathbf{u}) = 0. \tag{4.41}$$

Similarly, B_L and D_L can be defined as points satisfying

$$\lambda_s(\mathbf{u}_L) - s(\mathbf{u}_L, \mathbf{u}) = 0. \tag{4.42}$$

Therefore a slow compound wave C_1 can be defined as a rarefaction wave followed by a slow shock, consisting of a slow rarefaction wave and a jump to the point D_L. Similarly, a fast compound wave C_2 can be defined as a rarefaction wave followed by a fast shock, consisting of a jump to the point C_L and a fast rarefaction wave. For special left states at which C_L and D_L coincide, as found in Fig. 1(c), there is a possibility of a slow rarefaction followed by a shock to a fast rarefaction.

4.7. Solution of the Riemann problem

We study the Riemann problem for the planar 2×2 model:

$$\mathbf{u}_t + \mathbf{f}_x = 0, \tag{4.43}$$

$$\mathbf{u}(x, t = 0) = \begin{cases} \mathbf{u}_L & \text{if} \quad x \leqslant 0, \\ \mathbf{u}_R & \text{if} \quad x > 0. \end{cases}$$

The wave curve for a given state $\mathbf{u}_L$ is defined as the set of all states that can be connected to $\mathbf{u}_L$ by a single, physically relevant wave. In a sense, it is the union of the integral curves and the Hugoniot curves. However, we eliminate from the integral curves those branches that imply a steepening of the characteristics. Likewise, we

eliminate from the Hugoniot curves those branches that would imply characteristic divergence.

Close to $\mathbf{u}_L$, this is straightforward. In Fig. 6 we take $\mathbf{u}_L$ to be the points $L_{1,2,3,4,5}$, and we see departing from these points the slow (S_1) and fast (S_2) shock curves, along which u and λ both decrease, together with the slow (R_1) and fast (R_2) rarefaction curves, along which u and λ increase. We should also eliminate from the Hugoniot curves those shocks that are undercompressive, since these turn out to have unstable viscous profiles, and it needs to be noted that this branch includes the special point $u = u_L,\ v = -v_L$ corresponding to the Alfvén wave that rotates the transverse field through an angle π.

Finally, we need to add those states that can be reached through compound waves. These involve shocks that are on the border between regular and undercompressive shocks. This occurs when

$$s(\mathbf{u}_L, \mathbf{u}_R) = \lambda_1(\mathbf{u}_L), \quad \text{slow waves}, \quad s(\mathbf{u}_L, \mathbf{u}_R) = \lambda_2(\mathbf{u}_R), \quad \text{fast waves}.$$

Such shocks can be contiguous with rarefaction waves of the same family. The curve C_1 is defined by taking an arbitrary point $\mathbf{u}_M$ on R_1, and then finding the unique point $\mathbf{u}_N$ on the Hugoniot of $\mathbf{u}_M$ such that $s(\mathbf{u}_M, \mathbf{u}_N) = \lambda_1(\mathbf{u}_M)$. The curve C_2 is defined by finding the unique point $\mathbf{u}_K$ on the Hugoniot of $\mathbf{u}_L$ such that $s(\mathbf{u}_L, \mathbf{u}_K) = \lambda_2(\mathbf{u}_K)$ and then continuing the R_2 curve from $\mathbf{u}_K$.

To solve the Riemann problem, we take $\mathbf{u}_L$ to be fixed, and let $\mathbf{u}_R$ range over the phase space. Whenever $\mathbf{u}_R$ happens to lie on some branch of the wave curve for $\mathbf{u}_L$ the Riemann solution is simply the single wave indicated. That branch is therefore a boundary across which the other wave changes sign. Thus the regions either side of the S_1 wave curve correspond to wave patterns S_1R_1 or S_1S_2 and are so labelled. In Fig. 7, showing the exact solution of the planar Riemann problem, we denote these boundaries by continuous lines.

On a second type of boundary, one of the waves does not vanish, but changes character. This occurs when a compound wave becomes either a regular shock or a pure rarefaction. We denote these boundaries with dashed lines.

Finally, the O branch of the Hugoniot is a third kind of boundary, appearing in the middle of the S_1S_2 region. It corresponds to a limiting case in which the two shocks are parallel to each other, and merge to form a single overcompressive shock. It is shown, when it occurs, with a dotted line. Note that these waves required to solve the Riemann problem are precisely those admitted under the viscosity criterion.

Even though only two unknowns are involved, the reasoning involved in constructing the Riemann solution is intricate and not easy to formalize. Although we have independently verified the results of Schaeffer and Shearer (1987a) and Isaacson *et al.* (1988), *our method* consisted mostly of staring hard enough at the diagrams to become convinced that no case had been overlooked. We were, however, aided in doing this by the fact that for the model problem several theorems and analytical results are available.

4.8. Parallel limit

There are cases corresponding to parallel shocks, that is, shocks along the axis $\overline{v} = [v] = 0$. Such cases can be found in Figs 7(a,e). Their speed is given by $s = 2c\bar{u}$,

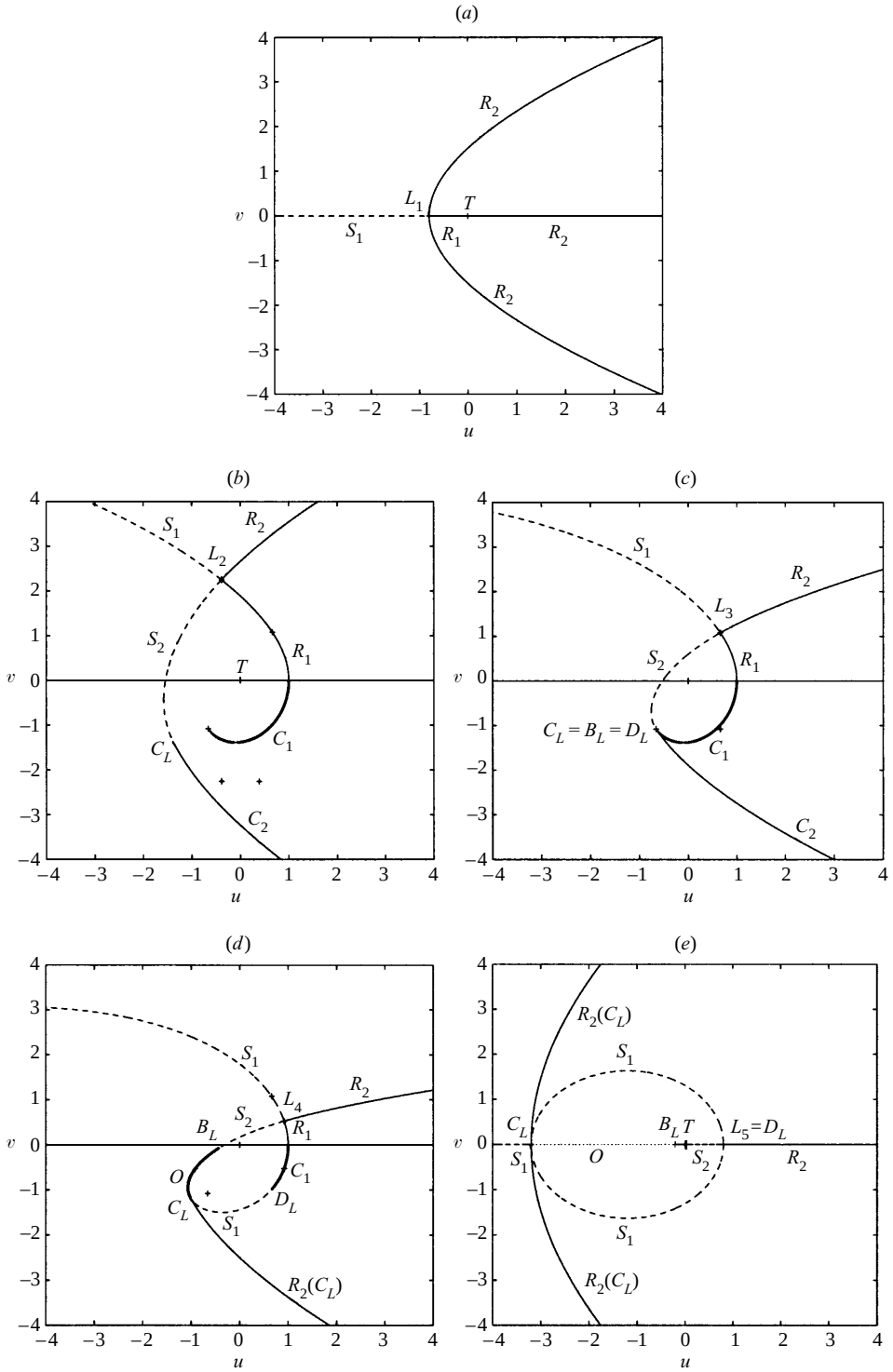

Figure 6. Wave curves. $R_2(C_L)$ denotes a fast rarefaction-wave curve originating from the point C_L.

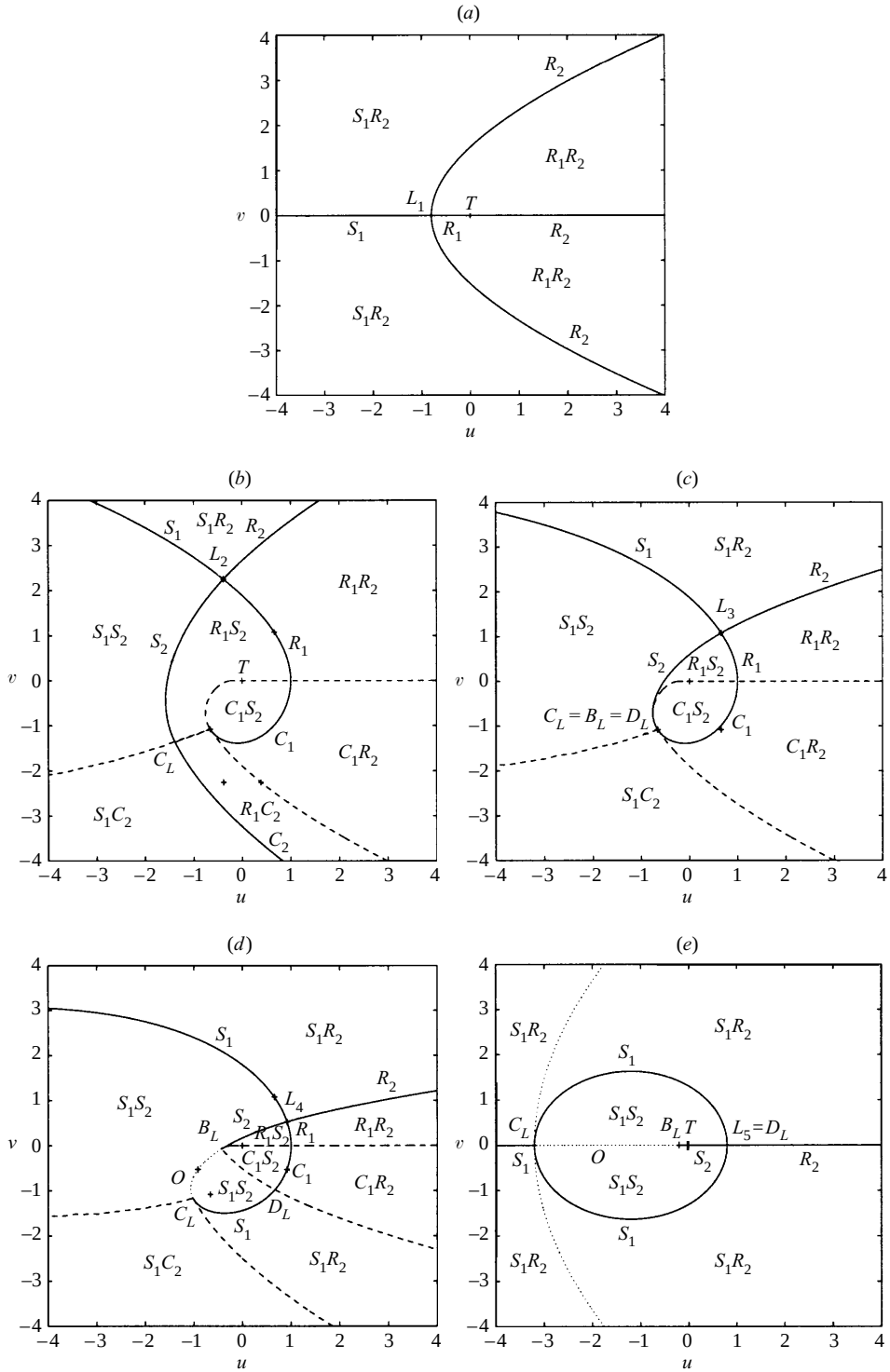

Figure 7. Exact solution of the Riemann problem: solid line, boundary line across which one wave is zero; dashed line, one wave changes character; dotted line, two waves coincide.

and they are overcompressive and physically relevant by the new theory if

$$0 < u_L, \quad \frac{c}{2-c}u_L < u < \frac{2-c}{c}u_L. \tag{4.44}$$

The overcompressive shocks in this limit have been considered non-physical by the evolutionary condition, resulting in the non-existence of solution. This shock is the same in physical space as the so-called *double-layer shocks*, that is, the combination of a switch-on and a switch-off shock (Jeffrey and Taniuti 1964, p. 258). Therefore the conventional theory is inappropriate for determining physically relevant shocks in MHD. In MHD, this case is investigated in Sec. 2.7 of Part 2 (Myong and Roe 1997).

5. Non-planar model system

Non-planar problems are of two types: coplanar problems with non-zero w components and non-coplanar problems. The distinction between the two types can be highlighted by introducing the transverse field moment defined as (Kennel *et al.* 1990)

$$I_z \equiv \int_{-\infty}^{\infty} w\, dx\,. \tag{5.1}$$

Starting from (3.7) and integrating them, we can derive the relation for the transverse field moment:

$$\frac{dI_z}{dt} + 2[uw] = 0\,. \tag{5.2}$$

When end states are coplanar, I_z is globally invariant. But once the problem becomes non-coplanar, I_z is no longer invariant, and is time-dependent.

In this section, keeping in mind the fundamental difference between the planar and non-planar problems, we shall explore the nonlinear evolution of intermediate shocks of the non-planar model. Most works are related to admissibility conditions, and the existence of viscous profiles. By investigating the singularity near the triple umbilic point, we shall demonstrate how the following argument of Keyfitz can be applied to the non-planar MHD Riemann problem (Keyfitz 1995, p. 579):

> One must begin with a careful statement of some physical basis for studying a Riemann problem, including a recognition that a theory centered on Riemann problems can apply only in a situation in which only self-similar solutions are to be expected. For example, this is the case if one is looking either at a very large time or a very small one.

This statement can be supported by the simple analysis that the conservation law is invariant under the scale transformation $x,\, t \to \alpha x,\, \alpha t$ and there exist two limits, $\alpha \to 0$ and $\alpha \to \infty$ (Glimm 1988). The former and the latter represent the instantaneous response to jump discontinuities and the large-time asymptotics respectively. Fortunately, it turns out in gasdynamics that both limits are not different. However, there is no reason why MHD must have the same property.

5.1. Rankine–Hugoniot relations

For the non-planar model, we have the following Rankine–Hugoniot conditions:

$$s[u] = 2c\bar{u}[u] + 2\bar{v}[v] + 2\bar{w}[w], \tag{5.3}$$

$$s[v] = 2\bar{v}[u] + 2\bar{u}[v], \tag{5.4}$$

$$s[w] = 2\bar{w}[u] + 2\bar{u}[w]. \tag{5.5}$$

Therefore the Hugoniot and wave trajectories are all either coplanar (v/w = const) or purely rotational (u = const, $s = 2\bar{u}$, $v^2 + w^2$ = const).

5.2. Shock waves

There appear three waves, which can be described using MHD terminology as slow, Alfvén and fast; their speeds are given by

$$\lambda_a = 2u, \qquad \lambda_{f,s} = (c+1)u \pm \{(c-1)^2u^2 + 4(v^2+w^2)\}^{1/2}, \tag{5.6}$$

always satisfying $\lambda_s \leqslant \lambda_a \leqslant \lambda_f$, and the right eigenvectors are

$$\mathbf{r}_a = \begin{pmatrix} 0 \\ w \\ -v \end{pmatrix}, \qquad \mathbf{r}_{f,s} = \begin{pmatrix} \frac{1}{2}\lambda_{f,s} - u \\ v \\ w \end{pmatrix}. \tag{5.7}$$

For a shock arising in the model system, the signs of the following six parameters determine which of the MHD characteristics run into the shock:

$$(\lambda_{f,a,s})_{L,R} - s. \tag{5.8}$$

In MHD terminology, the signs can be represented by four domains I–IV defined as

$$\text{IV} \quad \lambda_s \quad \text{III} \quad \lambda_a \quad \text{II} \quad \lambda_f \quad \text{I}.$$

There are 16 possible combinations, but only 12 can actually arise in the model system. IV $\rightarrow$ IV and I $\rightarrow$ I correspond to the right and left transport shocks, which turn out to be absent in the planar model. X(III $\rightarrow$ III) and X(II $\rightarrow$ II) correspond to the right and left transport shocks for Alfvén characteristics and it is not difficult to show that they are also absent in the model Hugoniot. A close look at the topology of the Hugoniot curves yields that there exist only three wave structures near undercompressive shocks ($S_2 - X - E_2$, $S_2 - X - E_1$, $S_1 - X - E_1$) and a special mode ($[u] = 0$, $s = 2\bar{u}$, $v^2 + w^2$ = const) can always be found in undercompressive shocks. Furthermore, it can be easily shown that signs of six parameters change only across this mode, and undercompressive shocks consist of II$\rightarrow$III and III$\rightarrow$II type shocks, depending on the sign of $[u]$. The 12 shocks are:

$$S_1\,(\text{II} \rightarrow \text{IV},\ \text{III} \rightarrow \text{IV}), \quad S_2\,(\text{I} \rightarrow \text{III},\ \text{I} \rightarrow \text{II}),$$

$$E_1\,(\text{IV} \rightarrow \text{II},\ \text{IV} \rightarrow \text{III}), \quad E_2\,(\text{III} \rightarrow \text{I},\ \text{II} \rightarrow \text{I}),$$

$$O\,(\text{I} \rightarrow \text{IV}), \quad E\,(\text{IV} \rightarrow \text{I}),$$

$$X\,(\text{II} \rightarrow \text{III},\ \text{III} \rightarrow \text{II}).$$

The relationship between the speed of a shock and waves in the 12 types of shocks is illustrated in Fig. 8. IS_1 and IS_2 denote intermediate slow and fast shocks. Because the classification is based only on the geometry of characteristics, we need to determine which shocks are physically meaningful.

5.3. Shock admissibility conditions

In Sec. 4.4, it is shown that the linear stability theory is inappropriate for the non-strictly hyperbolic system. Therefore, we will introduce the viscosity admissibility

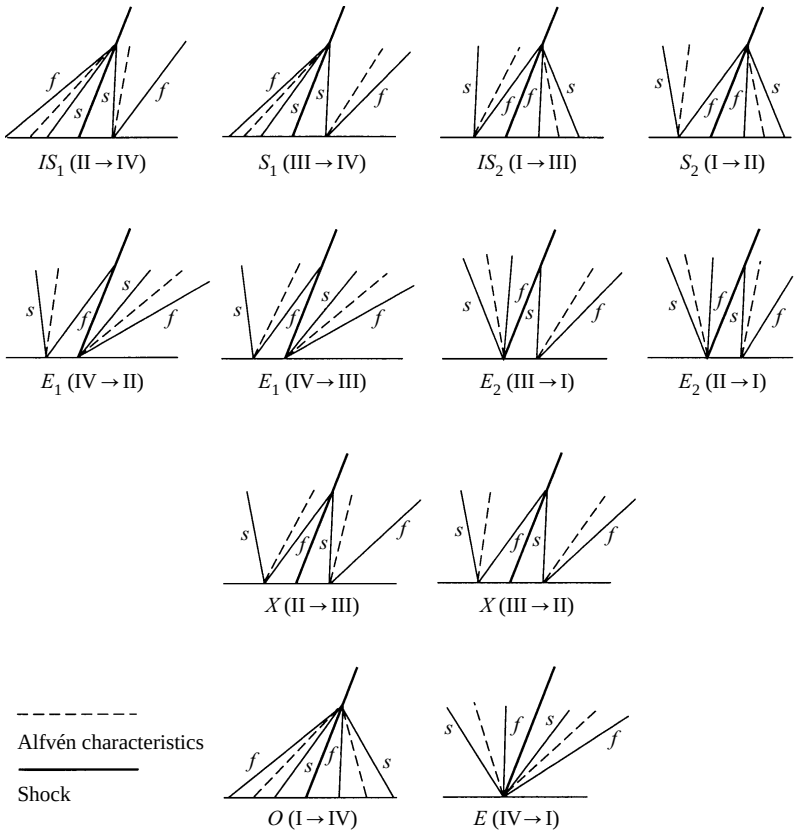

Figure 8. The relationship between the speed of a shock and characteristics. s and f represent families of slow and fast characteristics.

condition, and at the same time consider an entropy-flux condition since all viscous profiles are not necessarily stable in $n = 3$ system . Then we will show that admissible shocks of the non-planar model are regular shocks S_1 (III → IV), S_2 (I → II) and intermediate shocks IS_1 (II → IV), IS_2 (I → II), O (I → IV), X (II → III).

5.3.1. Evolutionary condition.. According to evolutionary theory, a discontinuity is evolutionary, in other words, physically relevant, if and only if the number of small-amplitude outgoing waves diverging from the discontinuity is equal to the number of the boundary conditions minus one. Or a travelling step discontinuity is called linearly dynamically stable if the linearized Rankine–Hugoniot equation has a unique solution for $t \geqslant 0$ (Freistühler 1992). The breakdown of this theory was shown by an example in Sec. 4.4.4.

The evolutionary condition restricts the permitted shocks to those having two diverging characteristics, that is, S_1 (III → IV), S_2 (I → II) and X (II → III). But, in order to ensure uniqueness, we need another condition on X (II → III) shocks since they can in general change u and $v^2 + w^2$ as well as the angle. Thus the only possible undercompressive shock is the so-called *rotational discontinuity*. In the framework of evolutionary theory, the Riemann solutions of the non-planar model consist of regular planar shocks and a rotational discontinuity. The relationship between the speed of evolutionary shocks and characteristics is summarized in

Figure 9. The relationship between the speed of evolutionary shocks and characteristics. In rotational discontinuity, characteristics of the same family are parallel to each other. In the diagram, a represents a family of Alfvén characteristics.

Fig. 9. The conclusion can be stated straightforwardly that the magnetic field can change its sign only through the rotational discontinuity.

5.3.2. An entropy condition.. For either the planar or non-planar systems there is a unique quadratic function that is conserved in smooth regions of the flow, and can serve as an entropy for the system. It is simply $e = \frac{1}{2}(u^2 + r^2)$, and in smooth regions it satisfies the conservation law

$$e_t + h_x = 0\,, \tag{5.9}$$

with an entropy flux $h = 2u(\frac{1}{3}cu^2 + r^2)$. Here, a vector $(v, w) = (r\cos\theta, r\sin\theta)$ is introduced. Across shocks, this entropy is dissipated, and it can be shown that

$$\frac{\partial}{\partial t}\int_{x_L}^{x_R} e\,dx = h(x_L) - h(x_R) + \tfrac{1}{2}[u]\{\tfrac{1}{3}c[u]^2 + [v]^2 + [w]^2\}. \tag{5.10}$$

For all compressive waves, $u_L > u_R$. Thus all compressive waves are entropy-dissipative. Note that no entropy dissipation is predicted for Alfvén waves.

When dissipation is included in the governing equations, the entropy evolution equation becomes

$$e_t + h_x = \mu(e_{xx} - u_x^2 - r_x^2 - r^2\theta_x^2). \tag{5.11}$$

Here μ and η are assumed to be equal. The first term in the parentheses leaves the entropy conserved, but the remaining terms dissipate it, including the last term which provides dissipation through rotation.

5.3.3. Viscous profiles.. By setting $\mu = \eta$ and $\chi = 0$, the dynamical system of the non-planar model system can be written as the ordinary differential equations

$$\begin{pmatrix} u \\ v \\ w \end{pmatrix}_{\xi} = \begin{pmatrix} cu^2 + v^2 + w^2 - ({cu_L}^2 + {v_L}^2 + {w_L}^2) - s(u - u_L) \\ 2(uv - u_L v_L) - s(v - v_L) \\ 2(uw - u_L w_L) - s(w - w_L) \end{pmatrix}. \tag{5.12}$$

The boundary conditions are

$$\lim_{\xi\to-\infty}\mathbf{u}(\xi) = \mathbf{u}_L, \quad \lim_{\xi\to\infty}\mathbf{u}(\xi) = \mathbf{u}_R, \quad \mathbf{u}_\xi(\pm\infty) = 0. \tag{5.13}$$

The travelling-wave solutions can exist only if $\mathbf{u}_{L,R}$ lie on the same Hugoniot curve, in which case they are also singular points of the ODE system. Therefore, for any non-coplanar Riemann problem involving changes of u and r, one cannot anticipate a single travelling-wave solution, because the Hugoniot curves are all either coplanar or purely rotational. For the coplanar problem, we can obtain the phase portrait of the 3×3 dynamical system by using the local approach. As for the planar problem, there are generally four singularities in finite domain, representing

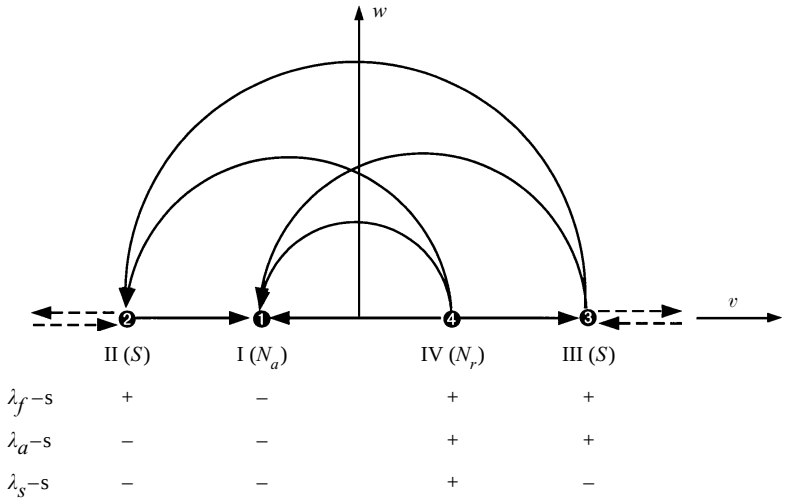

Figure 10. The phase portrait of the 3×3 system in the (v, w) domain. The dotted lines represent trajectories from singularities at infinity. Compare with examples of the phase portraits of the planar model.

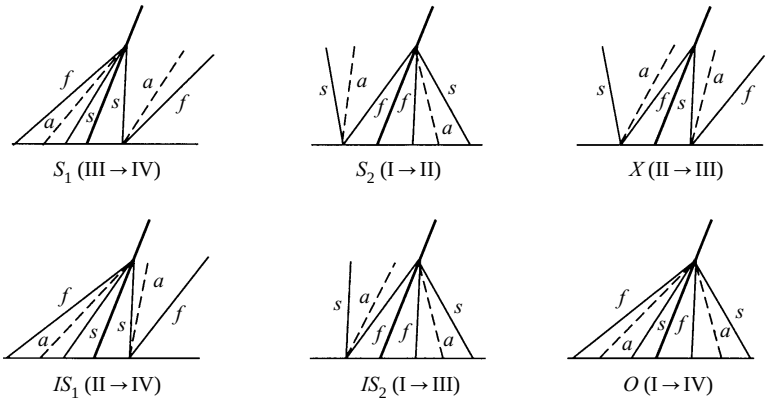

Figure 11. The relationship between the speed of shocks having viscous profiles and characteristics.

four reference state I–IV. Since the local topology near singularities depends on the sign of $\lambda_{f,a,s} - s$ and it must be identical with the phase portrait in planar limit, shown in Fig. 4, four states can be determined in the topology as

$$\mathrm{I}(N_a), \quad \mathrm{II}(S), \quad \mathrm{III}(S), \quad \mathrm{IV}(N_r).$$

A theory centred on Riemann problems can apply only in a situation in which only self-similar solutions are to be expected. For example, this is the case if one is looking either at a very large time or a very small one. A typical phase portrait is given in Fig. 10. It can be found that

$$\text{regular planar shocks (III} \to \text{IV, I} \to \text{II)}$$

and

$$\text{intermediate shocks (II} \to \text{IV, I} \to \text{III, I} \to \text{IV, II} \to \text{III),}$$

six in total, are physically admissible. Other shocks IV → II, IV → III, III → I, II → I, IV → I, and III → II are obviously inadmissible since they all do not have viscous profiles and violate the entropy-flux condition $[u] < 0$. In particular, the rotational discontinuities (which is a special case of II → III and III → II shocks) are inadmissible, since they contradict the inadmissibility of undercompressive shocks in the planar problem. The relationship between the speed of a shock and characteristics is summarized in Fig. 11.

On the other hand, we can obtain an *exact* solution for overcompressive and undercompressive shocks. It may be verified that

$$\left.\begin{aligned} u &= -u_0 \tanh\left(\frac{2u_0 x}{\mu}\right), \\ v &= -v_0 \tanh\left(\frac{2u_0 x}{\mu}\right) + Cw_0 \operatorname{sech}\left(\frac{2u_0 x}{\mu}\right), \\ w &= -w_0 \tanh\left(\frac{2u_0 x}{\mu}\right) - Cv_0 \operatorname{sech}\left(\frac{2u_0 x}{\mu}\right) \end{aligned}\right\} \tag{5.14}$$

is a solution of the system (5.12) for a stationary shock $s = 0$, provided that

$$C^2 = 1 + (c-2)\frac{u_0^2}{v_0^2 + w_0^2}.$$

Note that this solution satisfies the entropy-flux condition. This represents a viscous profile for an intermediate shock with $r_0^2 > (2-c)u_0^2$. The transverse vector rotates through the wave. In the (v, w) plane, it traces an ellipse whose major and minor axes are in the ration $C : 1$. Note that C can have either sign, corresponding to two senses of rotation around the ellipse. This special solution shows how the internal structure of an overcompressive shock can cause the rotation usually associated with Alfvén waves.

Without loss of generality, let $w_0 = 0$, so that the wave is polarized in the (x, y) plane. Then a transverse field moment

$$I_z = -C(\tfrac{1}{2}\mu\pi)\frac{v_0}{u_0}. \tag{5.15}$$

Initial data not satisfying this constraint must give rise to additional waves. An overcompressive shock necessarily satisfies $r_0 \leqslant c^{1/2}u_0$, so that $1 < 2(c-1)/c \leqslant C^2$.

In summary, for the non-planar problem, at least one family among the three families of characteristics converges across the physically admissible shocks.

5.4. Stability of intermediate shocks

5.4.1. Canonical cases.. For the coplanar problem, there is a jump across which $u \to -u, v \to -v$ and $w_{L,R} = 0$. Since $\bar{u} = \bar{v} = 0$, the Hugoniot relationships give $s = 0$. The wave speeds change according to

$$\lambda_{sR} = -\lambda_{fL}, \quad \lambda_{fR} = -\lambda_{sL}. \tag{5.16}$$

The wave is overcompressive if $\lambda_{sL} > 0$; this happens if $c^{1/2}u_L > v_L > 0$. Otherwise it is an undercompressive shock. Although such a jump satisfies the Hugoniot relationships, it decays into a pair of rarefaction waves, followed by a reversal shock along the line $c^{1/2}u_L = v_L$ in the planar limit. This special case of a reversal shock is called a *triple shock* (Isaacson *et al.* 1988). It can be regarded as a stationary slow

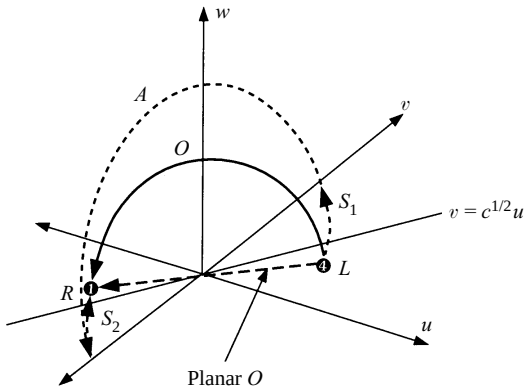

(*a*)

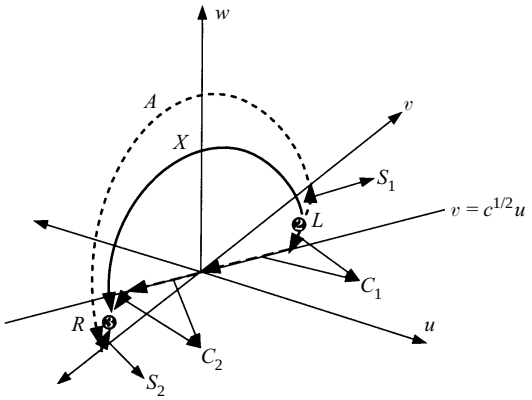

(*b*)

Figure 12. Riemann solutions in two canonical cases: (*a*) $0 < v_L < c^{1/2}u_L$; (*b*) $0 < c^{1/2}u_L < v_L$.

shock from $\mathbf{u} = \mathbf{u}_L$ to $\mathbf{u} = 0$, followed by a stationary fast shock from $\mathbf{u} = 0$ to $\mathbf{u} = \mathbf{u}_R$. Both of the component shocks and the overall jump satisfy the Hugoniot conditions. If the same data are presented to the restricted coplanar problem, u changes sign through shocks, but v does not. The solution is then a slow regular shock, followed by an Alfvén wave, and then a fast regular shock. The value of v_m in the Alfvén wave can be calculated from the Hugoniot relations as

$$\left.\begin{aligned} v_m &= \tfrac{1}{3}\{2(3cu_L^2 + 4v_L^2)^{1/2}\cos\tfrac{1}{3}\delta + v_L\}, \\ \delta &= \cos^{-1}\left(\frac{v_L\{(27-9c)u_L^2 - 8v_L^2\}}{(3cu_L^2 + 4v_L^2)^{3/2}}\right). \end{aligned}\right\} \tag{5.17}$$

Three different solutions in canonical cases are illustrated in Fig. 12, leading to *ill-posedness of the non-planar Riemann problem*. Introducing a non-dimensional parameter

$$I_z^* \equiv \frac{I_z}{\frac{1}{2}\pi\mu}, \tag{5.18}$$

we can compare I_z^* for three different solutions. Using (5.15) and (5.18), the follow-

ing relation is always satisfied:

$$I^*_{z\,\mathrm{planar}}(=0) \;<\; I^*_{z\,O,X} \;<\; I^*_{z\,S_1AS_2}. \tag{5.19}$$

In addition, we can calculate the rate at which the entropy is dissipated across the discontinuity. For the first case

$$\sum_{S_1,S_2} \frac{\partial E}{\partial t} \;<\; \left.\frac{\partial E}{\partial t}\right|_O, \tag{5.20}$$

and for the second case

$$\sum_{S_1,S_2} \frac{\partial E}{\partial t} \;<\; \left.\frac{\partial E}{\partial t}\right|_X \;<\; \sum_{C_1,C_2} \frac{\partial E}{\partial t}, \tag{5.21}$$

where $E \equiv \int_{-\infty}^{\infty} e\,dx$. Note that intermediate shocks experience the relatively high entropy dissipation rate.

5.4.2. Effect of non-coplanarity.. At the beginning of Sec. 5, we showed that once the problem becomes non-coplanar, I_z is no longer invariant, and is time-dependent. In this case the amount of I_z becomes infinite. In fact, the exact solution of planar Riemann problem given in Sec. 4.7 is valid only for sufficiently small I_z in the coplanar problem, and thus can be regarded as the neighbouring solution of the coplanar problem with large I_z and the non-coplanar problem near a rotation with angle π at a small time. Therefore we can deduce that intermediate shocks in the coplanar situation become time-dependent by any non-coplanar variation in the left and right states. As shown in canonical cases, an overcompressive shock is broken up into three waves, two regular shocks and a time-dependent intermediate shock, and eventually the intermediate shock becomes an Alfvén wave. From this analysis, we propose the following hypothesis.

Proposition 1. *Intermediate shocks are unstable under any non-coplanar variation on the upstream and downstream states, so that the large-time solution contains only regular planar shocks, but that intermediate shocks are needed to explain small-time behaviour.*

This hypothesis can be supported by observing that for very small non-coplanar variations, $dI_z/dt \approx 2\mu$, explaining that the solutions evolves in the direction of increasing I_z. It can also be confirmed by numerical experiment, for instance, using two-step Lax–Wendroff method with a very fine grid.

5.4.3. Nonlinear evolution.. From theoretical and numerical investigation of canonical cases, the nonlinear evolution of stationary overcompressive and undercompressive shocks can be summarized as in Fig. 13. In an overcompressive shock, the solution becomes planar O, coplanar O and S_1XS_2, in order of increasing I_z. When non-coplanar variations are applied, all have the same asymptotic solution S_1AS_2, which confirms Proposition 1 given above. In an undercompressive shock, the pattern becomes more complicated. The solution becomes planar C_1C_2, coplanar X and R_1XR_2, in order of increasing I_z. Finally, combining these results with the decrease of $\partial E/\partial t$ in order of increasing I_z and positive dI_z/dt for the non-coplanar situation, we may summarize the complicated pictures on nonlinear evolution of waves as follows.

In the planar problem, the evolution of waves can be described by the Riemann

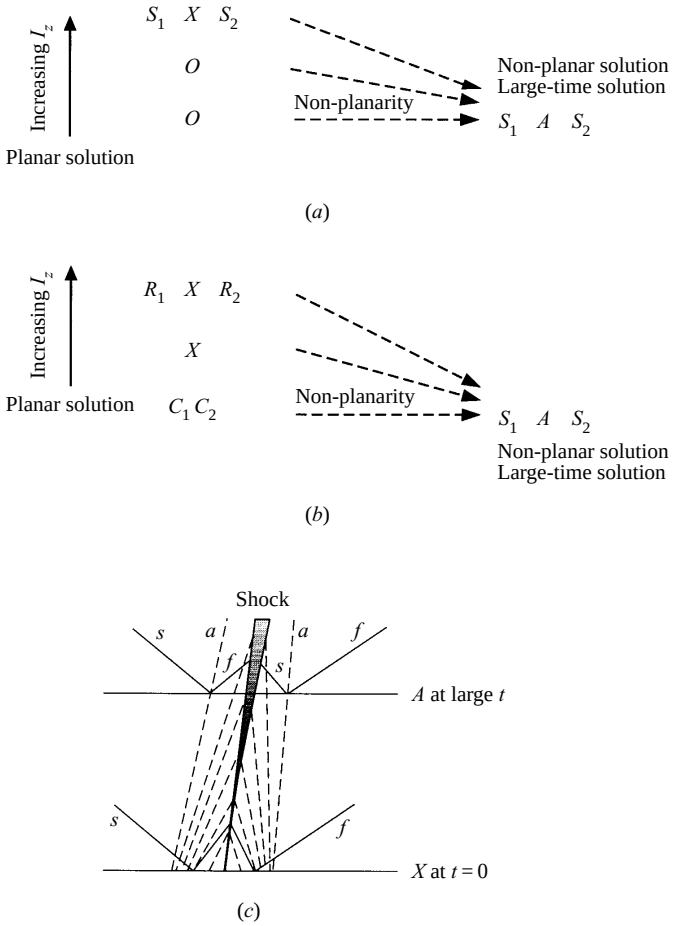

Figure 13. The evolution of stationary overcompressive and undercompressive shocks under external disturbances: (*a*) stability of a steady-state overcompressive shock (O); (*b*) stability of a steady-state undecompressive shock (X); (*c*) relationship between X and A and characteristics. Here A represents an Alfvén wave.

solutions, which are always self-similar. The associated shocks are time-independent and yield the maximum entropy-dissipation rate. In the coplanar problem, the evolution of waves becomes more complicated, since it depends on I_z. As in the planar problem, all shocks are time-independent. In the non-coplanar problem, the features of evolution of nonlinear waves can be distinguished largely in time: very small, intermediate and very large. At very small times, that is, before the viscosity works, the solutions are almost self-similar and associated waves are in general planar shocks and various time-dependent intermediate shocks. At intermediate times, that is, times during which the viscosity works actively, the Riemann solutions are not self-similar, so that time-dependent intermediate shocks evolve continuously (see also Wu 1994). Therefore in this region the evolution and structure of nonlinear shocks are highly coupled. At very large times, that is, after the effect of the viscosity has almost gone, only planar shocks survive, and all the complicated phenomena related to time-dependent intermediate shocks are gone, leaving a broad Alfvén wave.

5.4.4. Effect of dispersions.. Let us introduce $(\eta, \chi) = \mu' e^{i\psi}$ and $\sigma = \mu'/\mu$ where $-\frac{1}{2}\pi \leqslant \psi \leqslant \frac{1}{2}\pi$. Then the dynamical system of the non-planar model can be written as

$$D\begin{pmatrix} u \\ v \\ w \end{pmatrix}_{\xi} = \begin{pmatrix} [cu^2 + v^2 + w^2] - s[u] \\ [2uv]\cos\psi + [2uw]\sin\psi - s([v]\cos\psi + [w]\sin\psi) \\ -[2uv]\sin\psi + [2uw]\cos\psi - s(-[v]\sin\psi + [w]\cos\psi) \end{pmatrix}, \quad (5.22)$$

where

$$[Q] = Q - Q_L, \qquad D = \Big((1,0,0)^T, (0,\sigma,0)^T, (0,0,\sigma)^T\Big).$$

It can be shown that a class of data such that $\mathbf{u}_R = -\mathbf{u}_L$ and $s = 0$ is a singularity of the dynamical system. However, once non-coplanar variations are applied to the upstream and downstream states, intermediate shocks cannot persist as in the pure-dissipation case.

6. Concluding remarks

In this paper we have developed a framework that simplifies the study of the stability of global solutions, i.e., the study of the complicated phenomena of the evolution of MHD nonlinear waves. Our theory is based on the recent rigorous mathematical theory of non-strictly hyperbolic conservation laws, which has been successfully applied to various physical problems. The new theory is distinguished from conventional theories in that it is not self-contradictory, for example, it does not exhibit non-existence of solutions in the parallel limit. As a result, we could propose a new picture of the stability of MHD intermediate shocks, which has been a source of long-standing controversy in MHD. However, at the same time, we have found it very difficult to persuade those familiar with linearized stability theory to accept our viewpoint. Here we point out the following problems in conventional theory in the hope that they can help the reader see its weaknesses.

(i) The linearized stability theory is based on the assumption that the shock is weak, yet no one proved that all MHD shocks belong to such category. By contrast, as shown in Fig. 1, a shock cannot be assumed to be weak in the case of intermediate shocks. Thus the basis of the application of linearized stability theory is not justified in MHD.

(ii) An argument that needs only purely rotational, energy-dissipation free waves for changes in the direction of magnetic fields cannot describe correctly the process in collisional plasmas, since in such cases rotational waves always involve energy dissipation.

In consequence, linearized stability theory is self-contradictory and cannot correctly describe the evolution of MHD intermediate shocks.

In conclusion, the new theory can be summarized as follows. For physically relevant MHD shocks, first *at least* one family among the families of characteristics converges across the shocks, and secondly the entropy must increase by shocks. All of slow, fast planar and intermediate shocks and overcompressive shocks satisfy both conditions, but only some parts of undercompressive shocks do. By contrast, the evolutionary theory restricts such shocks to those across which *only* one family among the families of characteristics converges and to those by which the entropy does not decrease.

Acknowledgements

This work was supported in part by the National Science Foundation under Research Grant ATM-9318181. Also, R.S.M. wishes to thank the Korean Ministry of Education for its financial support in the initial stage of his graduate studies at the University of Michigan.

Appendix A. Theory of the dynamical system

A.1. The dynamical system

A dynamical system is determined by travelling-wave solutions to the associated parabolic equation. The dynamical system can be characterized by configurations in the phase space of an ordinary differential equation, because the configuration is related to the existence of a shock. Therefore analysis of the configuration is the essential tool for selecting shocks that admit a viscous profile.

The analysis of a system can be performed in the following steps. To derive a dynamical system, we start from the viscosity equation associated with conservation laws

$$\mathbf{u}_t + \mathbf{f}_x = \mathbf{D}\mathbf{u}_{xx}, \tag{A 1}$$

where we assume $\mathbf{u} = (u, v)$, $\mathbf{f} = (f(\mathbf{u}), g(\mathbf{u}))$, $\mathbf{D} = \mu\mathbf{I}$. Let $\mathbf{u}_L$ and $\mathbf{u}_R$ be two constant states connected by a shock with speed s. The travelling-wave solution of the form $\mathbf{u} = \mathbf{u}((x - st)/\mu = \xi)$ will converge to a weak solution of the given conservation laws. Then, by inserting $\mathbf{u} = \mathbf{u}(\xi)$, the viscosity equation reduces to

$$-s\mathbf{u}_\xi + \mathbf{f}_\xi = \mathbf{u}_{\xi\xi}, \tag{A 2}$$

and can be integrated once to yield

$$\mathbf{f}(\mathbf{u}) - \mathbf{f}(\mathbf{u}_L) - s(\mathbf{u} - \mathbf{u}_L) = \mathbf{u}_\xi. \tag{A 3}$$

In this process, the following boundary conditions must be satisfied:

$$\lim_{\xi\to-\infty} \mathbf{u}(\xi) = \mathbf{u}_L, \quad \lim_{\xi\to+\infty} \mathbf{u}(\xi) = \mathbf{u}_R. \tag{A 4}$$

This dynamical system may be regarded as a vector field X_s consisting of

$$u_\xi = f(\mathbf{u}) - f(\mathbf{u}_L) - s(u - u_L) \equiv \Theta(\mathbf{u}), \tag{A 5}$$

$$v_\xi = g(\mathbf{u}) - g(\mathbf{u}_L) - s(v - v_L) \equiv \Phi(\mathbf{u}). \tag{A 6}$$

Note that $\mathbf{u}_L$ and $\mathbf{u}_R$ are also singularities and that all singularities lie on the Hugoniot locus which is defined as

$$\{f(\mathbf{u}) - f(\mathbf{u}_L)\}(v - v_L) - \{g(\mathbf{u}) - g(\mathbf{u}_L)\}(u - u_L) = 0. \tag{A 7}$$

In general, singularities are determined by solving $\Theta = 0$ and $\Phi = 0$ for given s and $\mathbf{u}_L$. For instance, singularities on a finite domain are the intersections of two curves defined by $\Theta = 0$ and $\Phi = 0$. However, there is a special case in which $\mathbf{u}_L$ is the umbilic point, so that the eigenvalues become equal. In this case the Hugoniot locus is a straight line satisfying

$$\frac{f(u, v)}{u} = \frac{g(u, v)}{v}, \tag{A 8}$$

if we assume that $u_L = v_L = 0$. Singularities in this special case can be revealed by the Poincaré transform which is very useful for the analysis of unlimited orbits.

A.2. Poincaré transformation

An approach to examining the asymptotic behaviour of the unlimited orbits of a vector field is to use the so-called Poincaré transformation described below (Perko 1993, pp. 248–253). Consider the Poincaré sphere, where we project from the centre of the unit sphere $S^2 = \{(X, Y, Z) \in \mathbf{R}^3 \; | X^2 + Y^2 + Z^2 = 1\}$ onto the (x, y) plane tangent to S^2 at either the north or south pole. This projection has the advantage that the singular points at infinity are spread out along the equator of the sphere. If we project the upper hemisphere of the sphere onto the (x, y) plane, it follows that the equations defining (x, y) in terms of (X, Y, Z) are given by

$$x = \frac{X}{Z}, \quad y = \frac{Y}{Z}, \tag{A 9}$$

whereas the equations defining (X, Y, Z) in terms of (x, y) are given by

$$X = \frac{x}{(1 + x^2 + y^2)^{1/2}}, \quad Y = \frac{y}{(1 + x^2 + y^2)^{1/2}}, \quad Z = \frac{1}{(1 + x^2 + y^2)^{1/2}}. \tag{A 10}$$

These equations define a one-to-one correspondence.

A system $(\dot{x}, \dot{y}) = (P(x, y), Q(x, y))$ can be written in differential form as

$$Q(x, y)\, dx \; - P(x, y)\, dy = 0. \tag{A 11}$$

Let n denote the maximum degree of the terms in P and Q. Using the relation (A 9) and multiplying (A 11) by Z^n, the differential equation can be written as

$$\begin{vmatrix} dX & dY & dZ \\ X & Y & Z \\ P^* & Q^* & 0 \end{vmatrix} = 0, \tag{A 12}$$

where $P^*(X, Y, Z) = Z^n P(X/Z, Y/Z)$ and $Q^*(X, Y, Z) = Z^n Q(X/Z, Y/Z)$. Then, after some calculations, this leads a theorem summarized as follows: the flow in a neighborhood of any singular point of the system (A 12) on the equator of the sphere, except the points $(1, \pm 1, 0)$, is topologically equivalent to the flow defined by the system

$$\left.\begin{aligned} \dot{y} &= yz^n P(1/z, y/z) - z^n Q(1/z, y/z), \\ \dot{z} &= z^{n+1} P(1/z, y/z). \end{aligned}\right\} \tag{A 13}$$

Let $u \neq 0$. Applying $u = 1/z$ and $v = y/z$ to the vector field X_s and making the substitution $\zeta = z^n \xi$ (Gomes 1989), we get

$$\begin{aligned} \frac{dy}{d\zeta} &= -y\{-sz(1 - zu_L) + f(1, y) - z^2 f(u_L, v_L)\} \\ &\quad + g(1, y) - z^2 g(u_L, v_L) - sz(y - zv_L), \end{aligned} \tag{A 14}$$

$$\frac{dz}{d\zeta} = -y\{-sz(1 - zu_L) + f(1, y) - z^2 f(u_L, v_L)\}. \tag{A 15}$$

The points on the equator represent the points at infinity of the plane. So the singularities at infinity $(y, z = 0)$, if they exist, satisfy $-yf(1, y) + g(1, y) = 0$.

A.3. Local approach

Once we determine singularities in a finite domain, we can try to deal numerically with the dynamical system (A 5) and (A 6). The configuration of the dynamical system enables us to select admissible viscous profiles from all possible connections of singularities, since a viscous profile is a solution of the system subject to the boundary conditions $\Theta = \Phi = 0$ at each end point. But solving the dynamical system is a difficult and inefficient method, because it usually requires numerical integrations.

Instead, two alternatives may be used for the purpose of determining the type of singularity. The first is a local approach in which the local topology is defined by the sign of eigenvalues $\lambda_{f,s} - s$ of the matrix $\mathbf{A} - s\mathbf{I}$, where $\mathbf{A}$ is defined by $\partial\mathbf{f}/\partial\mathbf{u}$. This approach can be justified by the fact that the matrix is a tensor that relates the direction of the vector field u_ξ, v_ξ to a position within it. Thus a singularity can be classified as a repelling node if $\lambda_{f,s} > s$, an attracting node if $\lambda_{f,s} < s$, and a saddle if $\lambda_s < s < \lambda_f$.

A.4. Global approach (index theory)

The second approach is index theory (Perko 1993, pp. 273–290). This is a more rigorous, global analysis from the viewpoint of taking into account singularities at infinity. For a given vector field X_s on a two-dimensional surface, the index of a singularity can be defined as

$$I_{X_s}(C) = \frac{1}{2\pi} \oint_C d\tan^{-1}\left(\frac{dv}{du}\right), \tag{A 16}$$

where C is a piecewise-smooth simple, closed curve centred at the singularity. Thus the index is 1 at a node and -1 at a saddle, since a node can be represented by a vector field (u, v) or $(-u, -v)$, while a saddle can be described by $(u, -v)$. Furthermore, by the Poincaré index theorem, the sum of the indices of singularities on a two-dimensional surface is 2. Therefore we can easily determine the types of all singularities without resolving the orbits in detail.

References

Akhiezer, A. I., Akhiezer, I. A., Polovin, R. V., Sitenko A. G. and Stepanov, K. N. 1975 *Plasma Electrodynamics*, Vol. 1, *Linear Theory*. Pergamon Press, Oxford.

Akhiezer, A. I., Lubarski, G. J. and Polovin, R. V. 1959 The stability of shock waves in magnetohydrodynamics. *Soviet Phys. JETP* **8**, 507–511.

Akhiezer, A. I. and Polovin, R. V. 1960 The motion of a conducting piston in a magneto-hydrodynamic medium. *Soviet Phys. JETP* **11**, 383–386.

Bazer, J. and Ericson, W. B. 1958 Hydromagnetic shocks. *Astrophys. J.* **129**, 758–785.

Bell, J. B., Trangenstein, J. A. and Shubin, R. R. 1986 Conservation laws of mixed type describing three-phase flow in porous media. *SIAM J. Appl. Maths* **46**, 1000–1017.

Blokhin, A. M. 1994 *Strong Discontinuities in Magnetohydrodynamics*. NOVA, New York.

Bohachevsky, I. O. 1962 Simple waves and shocks in magnetohydrodynamics. *Phys. Fluids* **5**, 1456–1467.

Brio, M and Rosenau, P. 1994 Evolution and stability of the MHD fast-intermediate shock wave. Preprint.

De Hoffman, F. and Teller, E. 1950 Magneto-hydrodynamic shocks. *Phys. Rev.* **80**, 692–703.

Ericson, W. B. and Bazer, J. 1960 On certain properties of hydromagnetic shocks. *Phys. Fluids* **3**, 631–640.

Freistühler, H. 1992 Dynamical stability and vanishing viscosity: a case study of a non-strictly hyperbolic system. *Commun. Pure Appl. Maths* **45**, 561–582.

Glimm, J. 1988 The interaction of nonlinear hyperbolic waves. *Commun. Pure Appl. Maths* **41**, 569–590.

Gogosov, V. V. 1961 Resolution of an arbitrary discontinuity in magnetohydrodynamics. *J. Appl. Maths Mech.* **25**, 148–170.

Gomes, M. E. S. 1989 Riemann problem requiring a viscous profile entropy condition. *Adv. Appl. Maths* **10**, 285–323.

Holden, H. 1987 On the Riemann problem for a prototype of a mixed type conservation law. *Commun. Pure Appl. Maths* **40**, 229–264.

Isaacson, E. and Temple, B. 1988*a* The Riemann problem near a hyperbolic singularity II. *SIAM J. Appl. Maths* **48**, 1287–1301.

Isaacson, E. and Temple, B. 1988*b* The Riemann problem near a hyperbolic singularity III. *SIAM J. Appl. Maths* **48**, 1302–1312.

Isaacson, E., Marchesin, D., Plohr, B. and Temple, B. 1988 The Riemann problem near a hyperbolic singularity: the classification of solutions of quadratic Riemann problems I. *SIAM J. Appl. Maths* **48**, 1009–1031.

Isaacson, E., Marchesin, D. and Plohr, B. 1990 Transition waves for conservation laws. *SIAM J. Math. Anal.* **21**, 837–866.

Jeffrey, A. and Taniuti, A. 1964 *Non-Linear Wave Propagation.* Academic Press, New York.

Kantrowitz, A. R. and Petschek, H. E. 1966 MHD characteristics and shock waves. *Plasma Physics in Theory and Application* (ed. W. B. Kunkel), pp. 148–206. McGraw-Hill, pp. 148–206.

Kato, Y. and Taniuti, T. 1966 Propagation of hydromagnetic waves in collisionless plasma. I. *J. Phys. Soc. Japan* **21**, 765–777.

Kennel, C. F., Blandford, R. D. and Coppi, P. 1989 MHD Intermediate shock discontinuities. Part 1. Rankine–Hugoniot conditions. *J. Plasma Phys.* **42**, 299–319.

Kennel, C. F., Blandford, R. D. and Wu, C. C. 1990 Structure and evolution of small-amplitude intermediate shock waves. *Phys. Fluids* **B2**, 253–269.

Keyfitz, B. L. 1995 A geometric theory of conservation laws which change type. *Z. angew. Math. Mech.* **75**, 571–581.

Keyfitz B. L. and Kranzer, H. C. 1980 A system of hyperbolic conservation laws arising in elasticity theory. *Arch. Rat. Mech. Anal.* **72**, 219–241.

Kulikovskii, A. G. S. and Liubimov, G. A. 1961 On the structure of an inclined magneto-hydrodynamic shock wave. *J. Appl. Maths Mech.* **25**, 171.

Lax, P. 1957 Hyperbolic system of conservation laws II. *Commun. Pure. Appl. Maths* **10**, 537–566.

LeVeque, R. J. 1990 *Numerical Methods for Conservation Laws.* Birkhäuser, Basel.

Liu, H. 1992 The interactions of shock waves of nonstrictly hyperbolic systems. *Math. Acta Sci.* **12**, 312–336.

Myong, R. S. 1996 Theoretical and computational investigations of nonlinear waves in magnetohydrodynamics. PhD thesis, University of Michigan, Ann Arbor.

Myong, R. S. and Roe, P. L. 1997 Shock waves and rarefaction waves in magneto-hydrodynamics. Part 2. The MHD system. *J. Plasma Phys.* **58**, 521–552.

Perko, L. 1993 *Differential Equations and Dynamical Systems.* Springer-Verlag, New York.

Polovin, R. V.and Demutskii, V. P. 1990 *Fundamentals of Magnetohydrodynamics.* Consultants Bureau, New York.

Schaeffer, D. G. and Shearer, M. 1987*a* The classification of 2×2 systems of non-strictly hyperbolic conservation laws, with application to oil recovery. *Commun. Pure Appl. Maths* **40**, 141–178.

Schaeffer, D. G. and Shearer, M. 1987*b* Riemann problems for nonstrictly hyperbolic 2×2 systems of conservation laws. *Trans. Am. Math. Soc.* **304**, 267–306.

Shearer, M., Schaeffer, D. G., Marchesin, D. and Paes-Leme, P. J. 1987 Solution of the Riemann problem for a prototype 2×2 system of non-strictly hyperbolic conservation laws. *Arch. Rat. Mech. Anal.* **97**, 299–320.

Stakgold, I. 1979 *Green's Functions and Boundary Value Problems*. Wiley-Interscience, New York.

Sutton, G. W. and Sherman, A. 1965 *Engineering Magnetohydrodynamics*. McGraw-Hill, New York.

Web, G. M., Brio, M. and Zank, G. P. 1995 Symmetries of the triple degenerate DNLS equations for weakly nonlinear dispersive MHD waves. *J. Plasma Phys.* **54**, 201–244.

Wu, C. C. 1987 On MHD intermediate shocks. *Geophys. Res. Lett.* **14**, 668–671.

Wu, C. C. 1988*a* The MHD intermediate shock interaction with an intermediate wave: Are intermediate shocks physical? *J. Geophys. Res.* **93**, 987–999.

Wu, C. C. 1988*b* Effects of dissipation on rotational discontinuities. *J. Geophys. Res.* **93**, 3969–3982.

Wu, C. C. 1990 Formation, structure, and stability of MHD intermediate shocks. *J. Geophys. Res.* **95**, 8149–8175.

Wu, C. C. 1995 Magnetohydrodynamic Riemann problem and the structure of the magnetic reconnection layer. *J. Geophys. Res.* **100**, 5579–5598.

Wu, C. C. and Kennel, C. F. 1992 Evolution of small-amplitude intermediate shocks in a dissipative and dispersive system. *J. Plasma Phys.* **47**, 85–109.

Wu, C. C. and Kennel, C. F. 1993 The small amplitude magnetohydrodynamic Riemann problem. *Phys. Fluids* **B5**, 2877–2886.